



저작자표시-비영리-변경금지 2.0 대한민국

이용자는 아래의 조건을 따르는 경우에 한하여 자유롭게

- 이 저작물을 복제, 배포, 전송, 전시, 공연 및 방송할 수 있습니다.

다음과 같은 조건을 따라야 합니다:



저작자표시. 귀하는 원저작자를 표시하여야 합니다.



비영리. 귀하는 이 저작물을 영리 목적으로 이용할 수 없습니다.



변경금지. 귀하는 이 저작물을 개작, 변형 또는 가공할 수 없습니다.

- 귀하는, 이 저작물의 재이용이나 배포의 경우, 이 저작물에 적용된 이용허락조건을 명확하게 나타내어야 합니다.
- 저작권자로부터 별도의 허가를 받으면 이러한 조건들은 적용되지 않습니다.

저작권법에 따른 이용자의 권리는 위의 내용에 의하여 영향을 받지 않습니다.

이것은 [이용허락규약\(Legal Code\)](#)을 이해하기 쉽게 요약한 것입니다.

[Disclaimer](#)

理學碩士 學位論文

촉매와 불순물 도핑에 따른 ZnO 나노로드 성장  
양식에 관한 연구

**Effect of catalysts and dopants on the growth mechanism  
of *ZnO* nanorods**

指導教授 張志豪



2010年 2月

韓國海洋大學校 大學院

應用科學科 半導體物理專攻

吳承俊

理學碩士 學位論文

촉매와 불순물 도핑에 따른 ZnO 나노로드 성장  
양식에 관한 연구

**Effect of catalysts and dopants on the growth mechanism  
of *ZnO* nanorods**

指導教授 張志豪



2010年 2月

韓國海洋大學校 大學院

應用科學科 半導體物理專攻

吳承俊

本 論文을 吳承俊의 理學碩士 學位論文으로 認准함

위원장           李 三 寧 (인)

위 원           安 亨 秀 (인)

위 원           張 志 豪 (인)



2010 년 2 월

한국해양대학교 대학원

# Contents

논문 요약	1
Abstract	2
Figure list	3
Table list	7

## **Chapter 1. Introduction**

1.1) Introduction to nanostructures and nanomaterials	8
1.2) Various nanostructures	11
1.3) One dimensional nanostructures	15
1.4) Synthesis methods of one-dimensional nanostructure	17
1.4.1) Spontaneous growth	17
1.4.2) Electrospinning	18
1.4.3) Lithography	19
1.5) Proposal and organization of this thesis	21
REFERENCES	25

## **Chapter 2. Experiment and Theoretical background**

2.1) Synthesis of nanorods	29
2.2) Characterization of nanorods	30
2.2.1) Scanning Electron microscopy (SEM)	30

2.2.2) Energy dispersive X-ray spectroscopy (EDX)	33
2.3) Various growth mechanisms	36
2.3.1) Vapor-liquid-solid growth mechanism	37
2.3.2) Vapor-solid-solid growth mechanism	39
2.3.3) Solid-liquid-solid growth mechanism	41
2.3.4) Diffusion induced growth	42
REFERENCES	47

### **Chapter 3. Growth mechanism of ZnO nanorods on various catalyst**

3.1) Introduction	50
3.2) Experimental details	52
3.3) Characterization of ZnO nanorods on various catalyst	53
3.4) The effect of catalyst on growth of ZnO nanorods	56
3.5) Conclusion	59
REFERENCES	60

### **Chapter 4. Growth mechanism of Impurity doped ZnO nanorods**

4.1) Introduction	63
4.2) Experimental details	65
4.3) Characterization of In doped ZnO nanorods	66
4.4) The effect of dopants on growth of ZnO nanorods	69
4.5) Conclusion	70

REFERENCES	72
<b>Chapter 5. Conclusions</b>	75
<b>APPENDIX _ Magnitudes of Surface Energies</b>	78
<b>CURRICULUM VITAE</b>	81
<b>ACKNOWLEDGEMENTS</b>	85



## 논문요약

본 논문에서는 수평형 반응관을 이용하여 ZnO 나노로드를 제작함에 있어, 성장양식을 고찰하고 촉매의 종류와 불순물이 이 성장양식에 미치는 영향에 대해 고찰하였다. 본 논문은 총 5장으로 구성되어 있으며 각 장의 내용은 다음과 같다.

제1장에서는 나노구조와 나노물질에 대한 간략한 소개와 1차원의 나노구조, 그리고 ZnO 나노로드의 성장방법에 대해 소개하였다. 제2장에서는 제작된 ZnO 나노로드의 구조적 특성을 평가하기 위해 사용된 SEM과 불순물의 함량을 평가하기 위해 사용된 EDX에 대해서 자세히 소개하였고, 종래의 나노로드 성장양식에 관한 연구들을 정리하였다. 제3장에서는 금속촉매인 AuGe과 Ti을 사용하여 성장시킨 ZnO 나노로드에서 얻어진 데이터를 통해 이론적인 곡선과 비교하여, 촉매가 성장양식에 미치는 영향에 대해 고찰하였다. 제4장에서는 In이 도핑된 ZnO 나노로드를 성장하여 불순물이 성장양식에 미치는 영향에 대해 고찰하였다. 마지막으로 제5장에서는 본 논문에서 얻어진 결과를 정리하여 결론을 기술하였다.



## Abstract

In this thesis, ZnO nanorods were grown by using simple vertical vapor phase transportation (V-VPT) method. Growth mechanisms of ZnO nanorods grown with several kinds of catalysts and In dopants were investigated theoretically and experimentally.

In the chapter 1, a brief introduction of nanostructures and nanomaterials, 1D nanostructures and growth process of ZnO nanorods are described. The chapter 2 explains the principles of scanning electron microscopy (SEM) and energy dispersive X-ray spectroscopy (EDX). And also the previous studies on nanorods growth mechanism are reviewed. In the chapter 3, the effects of catalysts on the growth mechanism have been investigated. ZnO nanorods were grown by using different two catalysts (AuGe and Ti) and theoretical predictions were compared with experimental data. In the chapter 4, the growth mechanism of impurity doped ZnO nanorods was investigated. In the chapter 5, results were summarized and concluded.

# Figure list

## Chapter 1

**Figure 1.1.** The percentage of surface atoms changes with the palladium cluster diameter. 9

**Figure 1.2.** Schematic and scanning electron microscope (SEM) image of a gate electrode pattern on a GaAs/AlGaAs heterostructure used to create a quantum dot of complex shape in the underlying two-dimensional (2D) electron gas. (Courtesy of C. Marcus.) 10



**Figure 1.3.** (a) Low-magnification SEM image of the as-synthesized ZnO nanorings. (b) High-magnification SEM image of a freestanding single crystal ZnO nanoring, showing uniform and perfect geometrical shape. 12

**Figure 1.4.** SEM images of ZnO tubes. 13

**Figure 1.5.** SEM images of bunches of ZnO nanopropeller arrays. (a) a single column of the as-synthesized ZnO nanopropeller arrays; (b) front view of a column of ZnO nanopropeller arrays with nanowires at the central axis; (c) a column of ZnO nanopropeller arrays with uniform nanoribbon shape and

smoother surface; and (d) a column of ZnO nanopropeller arrays with long nanoribbons. 14

**Figure 1.6.** SEM image of ZnO:In nanocrystals with In-content of 8 at %. 15

**Figure 1.7.** Various 1D nanostructures. 16

**Figure 1.8.** Schematic procedures used for the preparation of single crystal silicon nanowires. 20

## Chapter 2

**Figure 2.1.** Schematic of the experimental setup for the growth of ZnO nanostructures. 30

**Figure 2.2.** Schematic describing the operation of an SEM. 33

**Figure 2.3.** A schematic of an EDX system on an electron column. The incident electron interacts with the specimen with the emission of X-rays. These X-rays pass thorough the window protecting the Si(Li) and are absorbed by the detector crystal. The X-ray energy is transferred to the Si(Li) and processed into a digital signal that is displayed as a histogram of number of photons versus energy. 35

**Figure 2.4.** Nanorod of material  $A$  of radius  $R$  and height  $H$  grown on the substrate activated by the drops of liquid alloy  $B+A$ . 38

**Figure 2.5.** Schematic depiction of Si nanorods growth by the SLS mechanism: (a) deposition of a thin layer of Ni on the Si(111) substrate; (b) formation of the Si–Ni eutectic liquid droplets; (c) continuous diffusion of Si atoms through the substrate–liquid (SL) interface into the liquid droplets, and growth of Si nanorods through the liquid–wire (LS) interface; (d) final state of Si nanorod growth. The smooth surface of the original substrate becomes rough at the end of Si nanorod growth. 42



**Figure 2.6.** The model of nanorod growth during VPT. Nanorod is assumed as being a cylinder of diameter  $D=2R$  and length  $L$ , the contact angle of drop is assumed to be  $90^\circ$ . 44

### Chapter 3

**Figure 3.1.** Cross-sectional SEM images of ZnO nanorods on various catalysts, the insets are plain-view image. (a) ZnO nanorods/Ti, and (c) ZnO nanorods/AuGe. 55

**Figure 3.2.** Experimental and theoretical length/diameter dependencies for (a) ZnO nanorods on Ti, (b) ZnO nanorods on AuGe. The theoretical curves are obtained from Eq. (2) in chapter 2. 57

## Chapter 4

**Figure 4.1.** Cross-sectional SEM images of ZnO:In nanorods/AuGe with different In composition, the insets are plain-view image. (a) Pure ZnO nanorods, (b) ZnO:In<sub>0.27</sub> nanorods and (c) ZnO:In<sub>0.33</sub> nanorods. 67

**Figure 4.2.** Experimental and theoretical length/diameter dependencies for (a) pure ZnO nanorods, (b) ZnO:In<sub>0.27</sub> nanorods and (c) ZnO:In<sub>0.33</sub> nanorods. The theoretical curves are obtained from Eq. (2) in chapter 2. 69

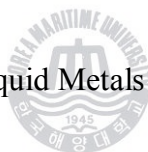
## Table list

**Table 1.1.** Various studies of the growth mechanisms of nanorods 22

**Table 3.1.** Various catalysts and growth methods of ZnO nanorods 51

**Table 4.1.** Various dopants of ZnO nanorods 64

**Table A.1.** Surface Tension of Liquid Metals 79



# Chapter 1. Introduction

## 1.1 Introduction to nanostructures and nanomaterials

Using the word “Nano” as a prefix for any unit like a second or a meter means a billionth of that unit. In nanotechnology, a widely accepted definition of nanomaterials is a system in which, at least, one dimension is nanometer scale. One nanometer is approximately the length equivalent to 10 hydrogen or 5 silicon atoms aligned in a line. Small features permit more functionality in a given space, but nanotechnology is not only a simple continuation of miniaturization from micron meter scale down to nanometer scale. At the nanoscale levels, materials have different physical, chemical and biological properties from the bulk. For example, crystals in the nanometer scale have a low melting point and reduced lattice constants, since the number of surface atoms or ions and the surface energy plays a significant role in the thermal stability. Crystal structures which are stable at high temperatures are stable at much lower temperatures in nanometer sizes. Nanostructures and nanomaterials possess a large fraction of surface atoms per unit volume. The ratio of surface atoms to internal atoms changes dramatically if one

successively divides a macroscopic object into smaller parts. Fig. 1.1 shows the percentage of surface atoms changes with the palladium cluster diameter.[1] Such a dramatic increase in the ratio of surface atoms to internal atoms in nanomaterials might illustrate why changes in the size range of nanometers are expected to lead to great changes in the physical and chemical properties of the materials. The changes of gold properties are considered as another example. Although bulk gold does not exhibit catalytic properties, Au nanocrystal demonstrates to be an excellent low temperature catalyst.

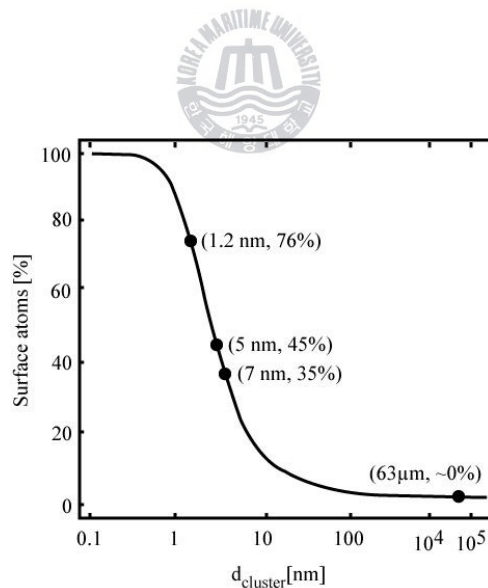


Fig.1.1. The percentage of surface atoms changes with the palladium cluster diameter.[1]



Many techniques have been developed in the synthesis and formation of these nanomaterials. The techniques for the creation of nanomaterials can be divided into two broad categories; top-down and bottom up approaches. Top-down approaches use lithographic patterning to structure macroscopic materials at the nanoscale, such as the metallic electrodes on top of a semiconductor heterostructure shown in Fig. 1.2.

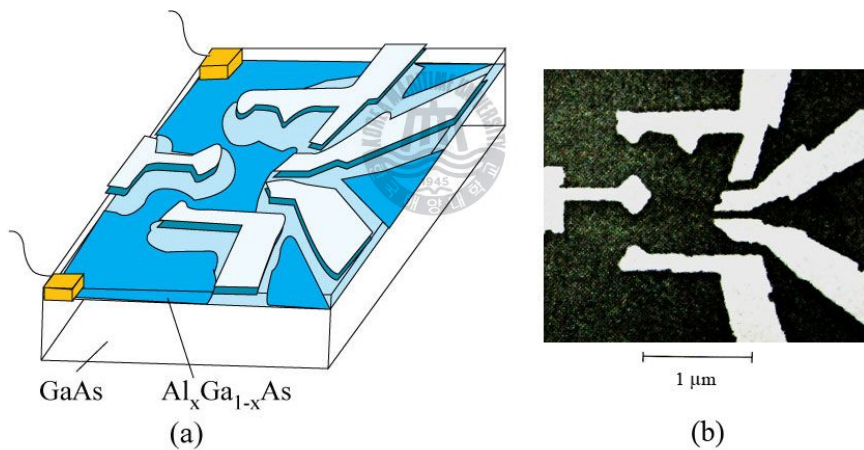


Fig. 1.2. Schematic and scanning electron microscope (SEM) image of a gate electrode pattern on a GaAs/AlGaAs heterostructure used to create a quantum dot of complex shape in the underlying two-dimensional (2D) electron gas. (Courtesy of C. Marcus.)

Spontaneous growth is considered as a bottom-up approach. Spontaneous growth generally results in the formation of single crystal nanomaterials along a preferential crystal growth direction depending on the crystal structures and surface properties of the nanomaterials. In order to produce and stabilize nanomaterials, it is essential to have a good understanding of surface energy and surface physical chemistry of solid surfaces. A major challenge of nanoscience and technology is to control the morphologies and properties over all length scales, from the molecular to the macroscopic.



## 1.2 Various nanostructures

A large number of publications have appeared lately reporting nanostructures of various shapes (nanobelts, nanorings, nanotubes, nanopropellers, nanotetrapods, etc.) grown by spontaneous growth under different growth condition. Nanobelts were considered for applications as nanosensors and nanoactuators, because the piezoelectric coefficient of a ZnO nanobelt was considerably larger than that for bulk ZnO.[2] Single-crystal nanorings of ZnO were grown by the solid-vapor process in a study by Kong *et al.*[3] Two types of nanoring structures

were found in their study. The type-I structure is the single-crystal entity nanoring with nearly perfect circular shape, although there is electron diffraction contrast caused by nonuniform deformation along the circumference. The type-II structure nanoring is a single crystal, which again implies that the nanoring shell is a uniformly deformed.

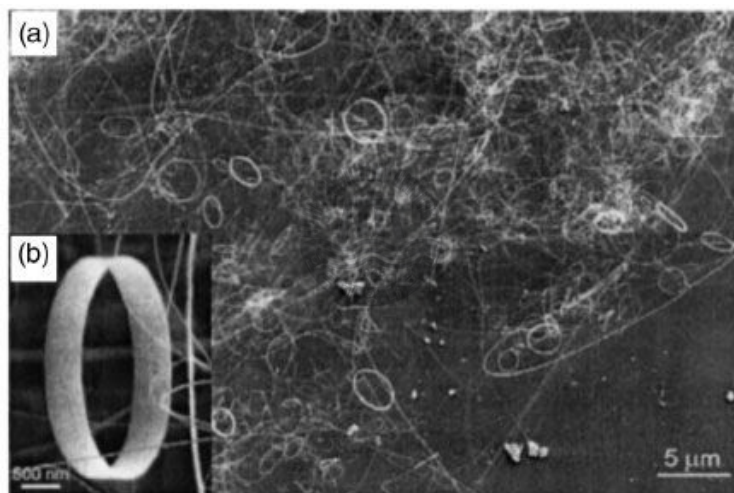


Fig. 1.3. (a) Low-magnification SEM image of the as-synthesized ZnO nanorings. (b) High-magnification SEM image of a freestanding single crystal ZnO nanoring, showing uniform and perfect geometrical shape.

ZnO nanotubes were synthesized by Zhang *et al.*[4] And also carbon

nanotubes (CNT) have been produced and observed under a variety of conditions. There is the reference for a review of the history of the discovery of carbon nanotubes.[5]

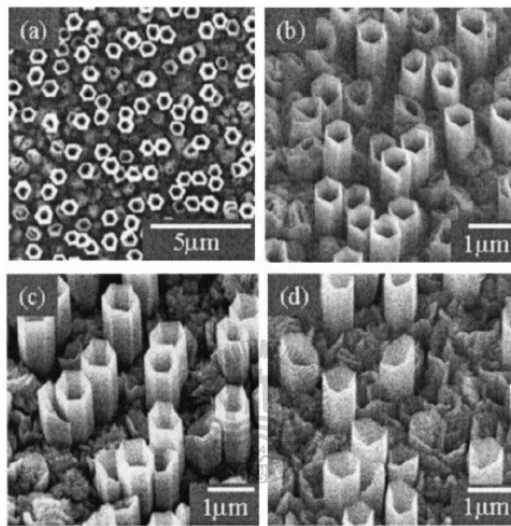


Fig. 1.4. SEM images of ZnO tubes.

As another example of various types of nanostructures, there are nanopropeller arrays and nanotetrapods. Nanopropeller arrays were synthesized using a two-step high-temperature solid-vapor deposition process by Gao and Wang.[6]

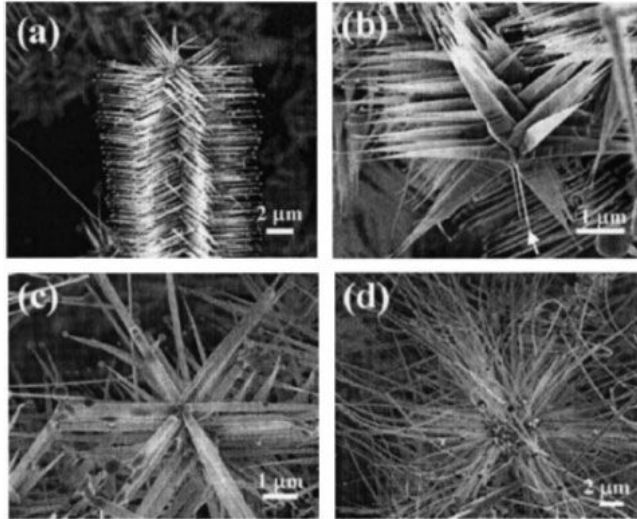


Fig. 1.5. SEM images of bunches of ZnO nanopropeller arrays. (a) a single column of the as-synthesized ZnO nanopropeller arrays; (b) front view of a column of ZnO nanopropeller arrays with nanowires at the central axis; (c) a column of ZnO nanopropeller arrays with uniform nanoribbon shape and smoother surface; and (d) a column of ZnO nanopropeller arrays with long nanoribbons.

Each nanopropeller array column consists of six arrays of triangular-shaped blades of 4–5  $\mu\text{m}$  in length and propeller arrays with a diameter of  $\sim 10 \mu\text{m}$ . The columns of the nanopropellers maintain their six-fold arrays of parallel nanoribbon blades around the central nanowire, as seen in Fig. 1.5(b).

Tetrapod-shape ZnO nanostructures were grown by vapor-phase

transportation without any assistance of catalyst.[7, 8] They demonstrated a novel field emission display (FED) by using these nanotetrapods.

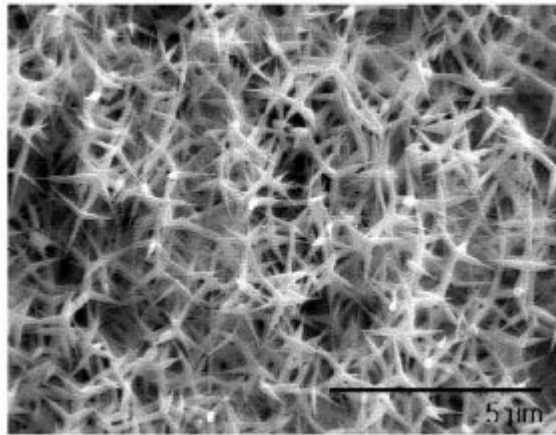


Fig. 1.6. SEM image of ZnO:In nanocrystals with In-content of 8 at %.

### 1.3 One dimensional nanostructures

One dimensional (1D) nanostructures have been called by a variety of names including: whiskers, fibers, nanowires and nanorods (Fig. 1.7). In many cases, nanotubes and nanocables are also considered one-dimensional structures. Since a discovery of CNT in 1991, 1D nanomaterials have attracted a high interest for years by the merits of their fascinating mechanical, electrical, optical and magnetic properties. However, it prevents CNT from being readily used for

applications that CNT has barriers such as difficulty in controlling the electronic properties of CNT and processing.

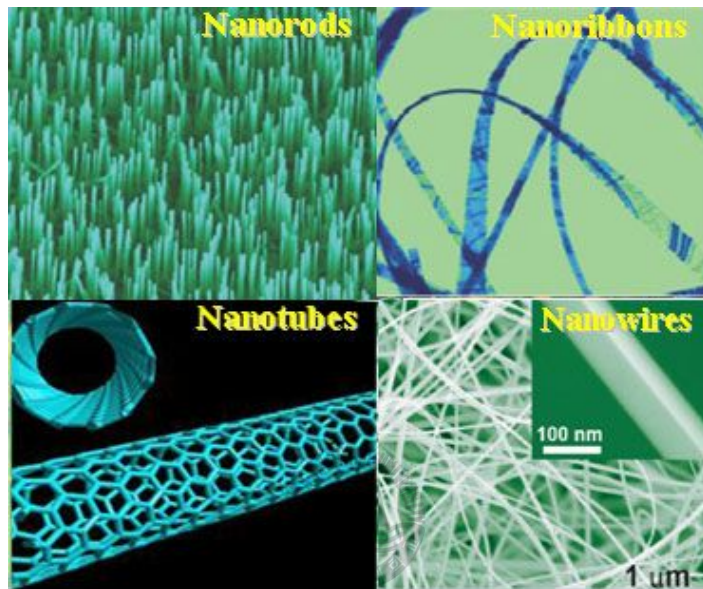


Fig. 1.7. Various 1D nanostructures.

Other than CNT, nanorods are ideal systems for investigating the dependence of electrical transport, optical and mechanical properties on size and dimensionality. They are expected to play an important role as both interconnects and functional components in the fabrication of nanoscale electronic and optoelectronic devices. Their unique and fascinating properties have already been

proposed or demonstrated for this class of materials, such as superior mechanical toughness, higher luminescence efficiency, enhancement of thermoelectric figure of merit, and a lowered lasing threshold.

For examples, Li *et al.*[8] reported that the high emission current density, high stability, and low turn-on field make the ZnO nanoneedle arrays one of the promising candidates for high brightness field-emission electron sources and flat-panel displays. And also, Könenkamp *et al.*[9] fabricated vertical nanowire LEDs using ZnO nanowires grown by electrodeposition from aqueous solutions on fluorine-doped SnO<sub>2</sub>-coated glass substrates.



In order to widen the application field, it is necessarily to control the dimension and shape of nanostructures. Various properties of nanorods are strongly related with the growth mode. Therefore, it is essential to understand the growth mechanism. Recently, many reports discussing the nanorod growth mechanism.

## **1.4 Synthesis methods of one-dimensional nanostructure**

### **1.4.1 Spontaneous growth**

Spontaneous growth is process driven by reduction of Gibbs free energy of



chemical potential. The reduction of Gibbs free energy is commonly realized by phase transformation or chemical reaction or the release of stress. For the formation of nanorods, anisotropic growth is required, i.e. the crystal grows along a certain orientation faster than other directions. Uniformly sized nanorods, i.e. the same diameter along the longitudinal direction of a given nanorods, can be obtained when crystal growth proceeds along one direction, whereas no growth along other directions. In spontaneous growth, for given material and growth conditions, defects and impurities in the growth surface can play an important role in determining the morphology of the final products.



#### **1.4.2 Electrospinning**

Electrospinning, also known as electrostatic fiber processing, technique has been originally developed for generating ultrathin polymer fibers.[10, 11] Electrospinning uses electrical forces to produce polymer fibers with nanometer-scale diameters. Electrospinning occurs when the electrical forces at the surface of a polymer solution or melt overcome the surface tension and cause an electrically charged jet to be ejected when the jet dries or solidifies, an electrically charged

fiber remains. This charged fiber can be directed or accelerated by electrical forces and then collected in sheets or other useful geometrical forms. More than 30 polymer fibers with diameters ranging from 40 nm to 500 nm have been successfully produced by electrospinning.[12, 13] The morphology of the fibers depends on the process parameters, including solution concentration, applied electric field strength, and the feeding rate of the precursor solution. Recently, electrospinning has also been explored for the synthesis of ultrathin organic-inorganic hybrid fibers.[14-17]



### **1.4.3 Lithography**

Lithography represents another route to the synthesis of nanowires. Various techniques have been explored in the fabrication of nanowires, such as electron beam lithography,[18, 19] ion beam lithography, STM lithography, X-ray lithography, and near-field photolithography.[20] Nanowires with diameter less than 10 nm and an aspect ratio of 100 can be readily prepared.

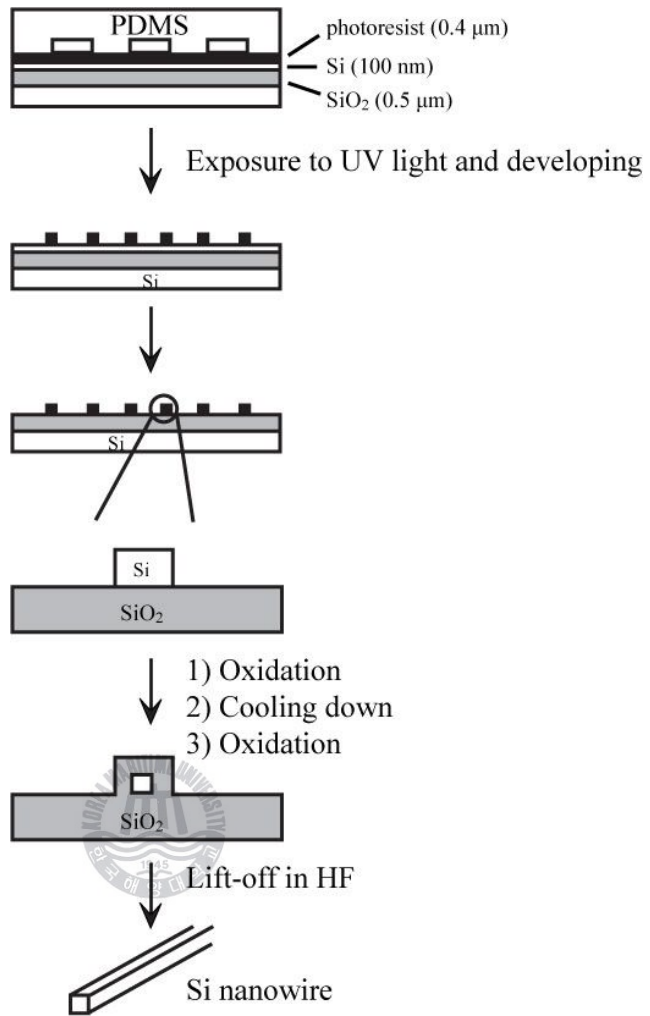


Fig. 1.8. Schematic procedures used for the preparation of single crystal silicon nanowires.[21]

Fig. 1.8 outlines the schematic procedures used for the preparation of single crystal silicon nanowire.[21] The nanoscale features were defined in a thin film of photoresist by exposing it to a UV light source through a phase shift mask

made of a transparent elastomer, such as poly (PDMS). The light passing through this phase mask was modulated in the near-field such that an array of nulls in the intensity was formed at the edges of the relief structures patterned on the PDMS mask. Therefore, nanoscale features were generated in a thin film of photoresist and the patterns were transferred into the underlying substrate using a reactive ion etching or wet etching process. Silicon nanostructures were separated from underlying substrate by slight over-etching.

## 1.5 Proposal and organization of this thesis



The applications of nanorods are diverse, ranging from display technologies to micro-electromechanical systems (MEMS). Among the wide variety of 1D semiconductor nanostructures, ZnO nanorods have received many attentions for optoelectronic nano-devices and sensing devices due to the simplest structural configuration. ZnO has been known as one of the representative materials in II-IV compound semiconductors. From the 1930s, ZnO have been studied. ZnO has a wide direct band-gap (3.37 eV) and a high exciton binding energy of 60 meV, which is suitable for efficient excitonic emissions and short wavelength in

optoelectronic application at room temperature.[22] Although there are such potential properties, a clear understanding on growth mechanism of nanorods is essential for controlling their potential properties. The growth mechanisms of nanorods have been studied for several decades (Table 1.1). Nevertheless there were many efforts, there remain many questions. For examples, although dopants are necessary for applying for electric or optoelectric devices,[23-25] but there are few studies on the effects of dopants on the growth mechanism of nanorods.

Table 1.1. Various studies of the growth mechanisms of nanorods

<b>Mechanisms</b>	<b>Ref</b>
Vapor-Liquid-Solid (VLS)	26-31
Vapor-Solid-Solid (VSS)	32-34
Vapor-Adsorption-Solid (VAdS)	32
Solid-Liquid-Solid (SLS)	35
Solution-Liquid-Solid (SLS)	36, 37
Supercritical-Fluid–Solid-Solid (SFSS)	37, 38

So far, ZnO nanorods have been grown through various apparatuses including metal organic vapor phase epitaxy (MOCVD), molecular beam epitaxy

(MBE), furnace, Hydro-thermal and so on. Among these methods, vapor phase transport and condensation (VPT) is the simplest and widely used method, which provides unique advantage in terms of the controllability of nanostructure.

In this study, I have grown the vertically well-aligned ZnO nanorods by using simple vertical vapor phase transportation (V-VPT) method. The aim of this work is theoretical and experimental investigation of ZnO nanorods grown with several kinds of catalysts and In dopants by VPT process. This work will be an important guidance for the improved controllable growth of nanorods, also it enables a development of novel nano-device with high performance.



The chapter 2 describes the growth method of nanorods using VPT and introduces various measurements, such as scanning electron microscopy (SEM), and energy dispersive X-ray spectroscopy (EDX) to investigate the grown ZnO nanorods. And various growth mechanisms of nanorods will be reviewed. In the chapter 3, the growth mechanism of ZnO nanorods grown on various catalysts will be investigated. Adatom kinetic behaviors on various catalysts will be discussed. The chapter 4 is focused on the growth mechanism of impurity doped ZnO nanorods. Doping is inevitable for the application of nanostructures to electric or

optoelectric devices, so it is worthy to investigate on the effect of dopants. In the chapter 5, summary and conclusion will be given.



## REFERENCES

- [1] Nanostructures p.16. C. Nutzenadel, A. Zuttel, D. Chartouni, G. Schmid, and L. Schlapbach, *Eur. Phys. J. D8*, 245 (2000).
- [2] M.H. Zhao, Z.L. Wang, and S.X. Mao, *Nano Lett.* 4, 587 (2004).
- [3] X.Y. Kong, Y. Ding, R. Yang, and Z.L. Wang, *Science* 303, 1348 (2004).
- [4] B.P. Zhang, N.T. Binh, K. Wakatsuki, Y. Segawa, Y. Yamada, N. Usami, M. Kawasaki, and H. Koinuma, *Appl. Phys. Lett.* 84, 4098 (2004).
- [5] Monthieux, Marc; Kuznetsov, Vladimir L. "Who should be given the credit for the discovery of carbon nanotubes?". *Carbon* 44, 1621 (2006).
- [6] P.X. Gao and Z.L. Wang, *Appl. Phys. Lett.* 84, 2883 (2004).
- [7] M.N. Jung, S.H. Park, S.Y. Ha, S.J. Oh, Y.R. Cho, J.S. Park, I.H. Im, B.H. Koo, T. Yao, and J.H. Chang, *Physica E* 40, 2761 (2008).
- [8] Y.B. Li, Y. Bando, and D. Golberg, *Appl. Phys. Lett.* 84, 3603 (2004).
- [9] R. Könenkamp, R.C. Word, and C. Schlegel, *Appl. Phys. Lett.* 85, 6004 (2004).
- [10] A. Frenot and I.S. Chronakis, *Current Opin. Colloid Interf. Sci.* 8, 64 (2003).
- [11] D.H. Reneker and I. Chun, *Nanotechnology* 7, 216 (1996).



- [12] H. Fong, W. Liu, C.S. Wang, and R.A. Vaia, *Polymer* 43, 775 (2002).
- [13] J.A. Mathews, G.E. Wnek, D.G. Simpson, and G.L. Bowlin, *Biomacromolecules* 3, 232 (2002).
- [14] G. Larsen, R. Velarde-Ortiz, K. Minchow, A. Barrero, and I.G. Loscertales, *J. Am. Chem. Soc.* 125, 1154 (2003).
- [15] H. Dai, J. Gong, H. Kim, and D. Lee, *Nanotechnology* 12, 674 (2002).
- [16] D. Li and Y. Xia, *Nano Lett.* 3, 555 (2003).
- [17] D. Li and Y. Xia, in *Nanomaterials and Their Optical Applications*, *SPIE Proceedings* 5224 (2003).
- [18] K. Kurihara, K. Iwadate, H. Namatsu, M. Nagase, and K. Murase, *J. Vac. Sci. Technol.* B13, 2170 (1995).
- [19] H.I. Liu, D.K. Biegelsen, F.A. Ponce, N.M. Johnson, and R.F. Pease, *Appl. Phys. Lett.* 64, 1383 (1994).
- [20] Y. Xia, J.A. Rogers, K.E. Paul, and G.M. Whitesides, *Chem. Rev.* 99, 1823 (1999)
- [21] Y. Yin, B. Gates, and Y. Xia, *Adv. Mater.* 12, 1426 (2000).
- [22] D.C. Reynolds, D.C. Look, B. Jogai et al, *J. Appl. Phys.* 88, 2152 (2002).



- [23] C.L. Hsin, J.H. He, and L.J. Chen, *Appl. Phys. Lett.* 88, 063111 (2006).
- [24] Y.J. Li, M.Y. Lu, C.W. Wang, K.M. Li, and L.J. Chen, *Appl. Phys. Lett.* 88, 143102 (2006).
- [25] J. Zhong, S. Muthukumar, Y. Chen, Y. Lu, H.M. Ng, W. Jiang and E.L. Garfunkel, *Appl. Phys. Lett.* 83, 3401 (2003).
- [26] R.S. Wagener and W.C. Ellis, *Appl. Phys. Lett.* 4, 89 (1964).
- [27] E.I. Givargizov, *J. Cryst. Growth* 31, 20 (1975).
- [28] V.G. Dubrovskii and N.V. Sibirev, *Phys. Rev. E* 70, 031604 (2004).
- [29] V.G. Dubrovskii, G.E. Cirlin, I.P. Soshnikov, A.A. Tonkikh, N.V. Sibirev, Y.B. Samsonenko, and V.M. Ustinov, *Phys. Rev. B* 71, 205325 (2005).
- [30] V.G. Dubrovskii, I.P. Soshnikov, N.V. Sibirev, G.E. Cirlin, and V.M. Ustinov, *J. Cryst. Growth* 289, 31 (2006).
- [31] V.G. Dubrovskii and N.V. Sibirev, *J. Cryst. Growth* 304, 504 (2007).
- [32] G.A. Bootsma, and H.J. Gassen, *J. Cryst. Growth* 10, 223 (1971).
- [33] T.I. Kamins, R.S. Williams, D.P. Basile, T. Hesjedal, and J.S. Harris, *J. Appl. Phys.* 89, 1008 (2001).
- [34] A.I. Persson, M.W. Larsson, S. Stenström, B.J. Ohlsson, L. Samuelson, and

L.R. Wallenberg, *Nat. Mater.* 3, 677 (2004).

- [35] a) D.P. Yu, Y.J. Xing, Q.L. Hang, H.F. Yan, J. Xu, Z.H. Xi, and S.Q. Feng, *Phys. E* 9, 305 (2001). b) A. Gorbunov, O. Jost, W. Pompe, and A. Graff, *Carbon* 40, 113 (2002). c) H.F. Yan, Y.J. Xing, Q.L. Hang, D.P. Yu, Y.P. Wang, J. Xu, Z.H. Xi, and S.Q. Feng, *Chem. Phys. Lett.* 323, 224 (2000).
- [36] a) T.J. Trentler, K.M. Hickman, S.C. Goel, A.M. Viano, P.C. Gibbons, and W.E. Buhro, *Science* 270, 1791 (1995). b) Y.P. Fang, X.G. Wen, S.H. Yang, and *Angew. Chem. Int. Ed.* 45, 4655 (2006).
- [37] F.M. Davidson, D.C. Lee, D.D. Fanfair, and B.A. Korgel, *J. Phys. Chem. C.* 111, 2929 (2007).
- [38] H.Y. Tuan, D.C. Lee, T. Hanrath, and B.A. Korgel, *Nano Lett.* 5, 681 (2005).

## Chapter 2. Experiment and Theoretical background

### 2.1 Synthesis of nanorods

In general the properties and growth mechanism of the nanorods are closely related with the diffusion and transportation of material on the crystalline surfaces. They depend upon the pressure and temperature of the system also the chemical environment and reaction kinetics. The kinetic behavior of the nuclei is also important. Therefore, there were many researches on the growth methods including the various growth chamber design and geometry for each material.



In this study, ZnO nanorods were grown by using the horizontal tube furnace which is a kind of furnace apparatus. The principle way of nanorod growth in a horizontal tube furnace is basically vapor phase transport and condensation (VPT). The gold transparent electric furnace is as shown schematically in Fig. 2.1. The source boat, which is loaded with both sources and a substrate, was placed at the center of the quartz reactor equipped with the inner tube. The tubes and trays are generally made of quartz or alumina due to their excellent durability against high temperature. The furnace has many merits. For example, operating is the

simplest among other apparatuses. It can be easily reformed to fit with the condition of system.

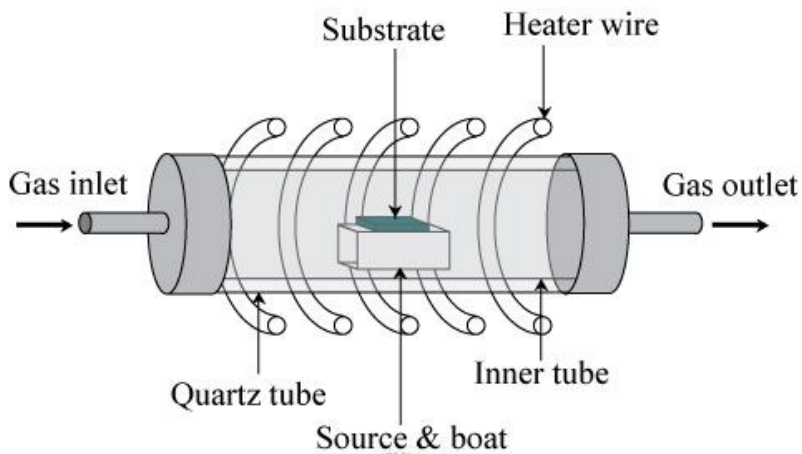


Fig. 2.1. Schematic of the experimental setup for the growth of ZnO nanostructures.

## 2.1 Characterization of nanorods

### 2.2.1 Scanning electron microscope (SEM)

Scanning electron microscope (SEM) has become one of the most versatile and useful method for direct imaging, characterization, and studying on structural properties of nanorods. The resolution of the SEM approaches several nanometers, and the instruments can operate at magnifications that are easily adjusted from  $\sim 10$  to over 300,000. In a general SEM, a source of electrons is focused into a beam,

with a very fine spot of  $\sim 5$  nm and having energy ranging from a few hundred eV to 50 keV. As the electrons strike and penetrate the surface, a number of interactions occur that result in the emission of electrons and photons from the sample, and SEM images are produced by collecting the emitted electrons on a cathode ray tube (CRT). Various SEM techniques are differentiated on the basis of what is subsequently detected and imaged, and the principle images produced in the SEM are of three types: secondary electron images, backscattered electron images and elemental X-ray maps. When a high-energy primary electron interacts with an atom, it undergoes either inelastic scattering with atomic electrons or elastic scattering with the atomic nucleus. In an inelastic collision with an electron, the primary electron transfers part of its energy to the other electron. When the energy transferred is large enough, the other electron will emit from the sample. If the emitted electron has energy of less than 50 eV, it is referred to as a secondary electron. Backscattered electrons are the high-energy electrons that are elastically scattered and essentially possess the same energy as the incident or primary electrons. The probability of backscattering increases with the atomic number of the sample material. Although backscattering images cannot be used for elemental



identification, useful contrast can develop between regions of the specimen that differ widely in atomic number,  $Z$ . An additional interaction in the SEM is that the primary electron collides with and ejects a core electron from an atom in the sample. The excited atom will decay to its ground state by emitting either a characteristic X-ray photo or an Auger electron, both of which have been used for chemical characterization and will be discussed later in this chapter. Combining with chemical analytical capabilities, SEM not only provides the image of the morphology and microstructures of bulk and nanostructured materials and devices, but can also provide detailed information of chemical composition and distribution.



The theoretical limit to an instrument's resolving power is determined by the wavelengths of the electron beam used and the numerical aperture of the system.

The resolving power,  $R$ , of an instrument is defined as:

$$R = \frac{\lambda}{2NA}$$

Where  $\lambda$  is the wavelength of electrons used and  $NA$  is the numerical aperture, which is engraved on each objective and condenser lens system, and a measure of the electron gathering ability of the objective, or the electron providing ability of the condenser.[1]

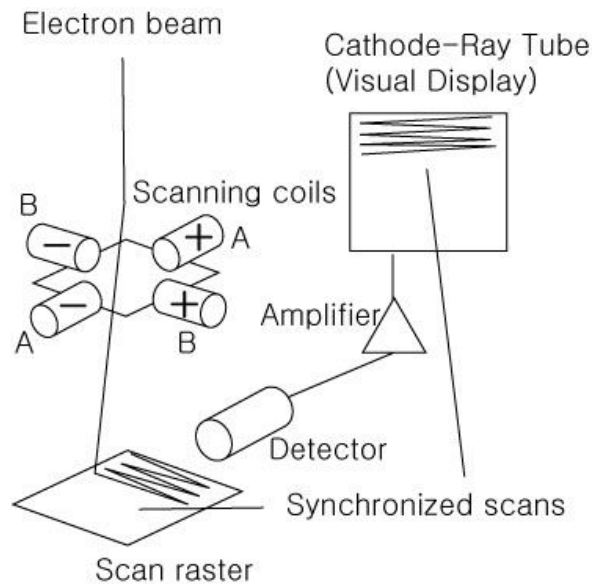


Fig. 2.2. Schematic describing the operation of an SEM



### 2.2.2 Energy dispersive X-ray spectroscopy (EDX)

Energy-dispersive X-ray spectroscopy (EDX) has been used for quality control and test analysis in many industries including: computers, semiconductors, metals, cement, paper, and polymers. EDX has been used in medicine in the analysis of blood, tissues, bones, and organs; in pollution control, for asbestos identification; in field studies including ore prospecting, archeology, and oceanography; for identification and forgery detection in the fine arts; and for



forensic analysis in law enforcement. With a radioactive source, an EDX system is easily portable and can be used in the field more easily than other spectroscopy techniques. The main advantages of EDX are its speed of data collection; the detector's efficiency (both analytical and geometrical); the ease of use; its portability; and the relative ease of interfacing to existing equipment.

X-rays are produced as a result of the ionization of an atom by high energy radiation wherein an inner shell electron is removed. To return the ionized atom to its ground state, an electron from a higher energy outer shell fills the vacant inner shell and, in the process, releases an amount of energy equal to the potential energy difference between the two shells. This excess energy, which is unique for every atomic transition, will be emitted by atom either as an X-ray photon or will be self-absorbed and emitted as an Auger electron.

As shown Fig. 2.3, the heart of the EDX is a diode made from a silicon crystal with lithium atoms diffused, or drifted, from one end into the matrix. The lithium atoms are used to compensate the relatively low concentration of grown-in impurity atoms by neutralizing them. In the diffusion process, the central core of the silicon will become intrinsic, but the end away from the lithium will remain p-

type and the lithium end will be n-type. The result is a p-i-n diode.

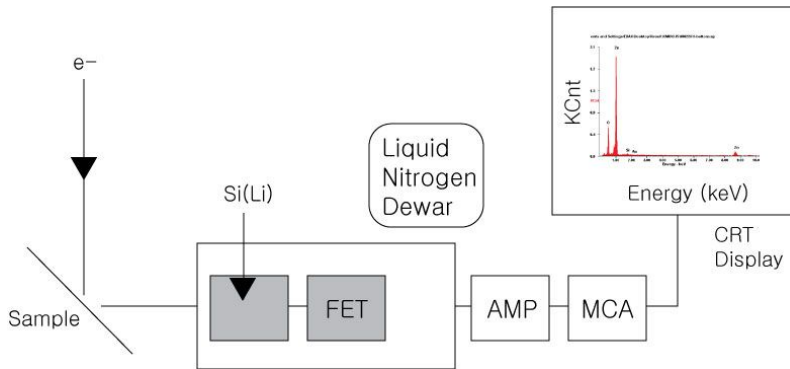


Fig. 2.3. A schematic of an EDX system on an electron column. The incident electron interacts with the specimen with the emission of X-rays. These X-rays pass through the window protecting the Si(Li) and are absorbed by the detector crystal. The X-ray energy is transferred to the Si(Li) and processed into a digital signal that is displayed as a histogram of number of photons versus energy.

When an X-ray photon enters the intrinsic region of the detector through the p-type end, there is a high probability that it will ionize a silicon atom through the photoelectric effect. This results in an X-ray or an Auger electron, which in turn produces a number of electron-hole pairs in the Si(Li). Both charge carriers move freely through the lattice and are drawn to the detector contacts under the action of

the applied bias field to produce a signal at the gate of a specially designed field effect transistor mounted directly behind the detector crystal. The transistor forms the input stage of a low-noise charge-sensitive preamplifier located on the detector housing. The output from the preamplifier is fed to the main amplifier, where the signal is finally amplified to a level that can be processed by the analog-to-digital converter (ADC) of the multi channel analyzer (MCA). The height of the amplifier output pulse is proportional to the input preamplifier pulse, and hence is proportional to the X-ray source.



### **2.3 Various growth mechanisms**

Nanorods are rod like nanocrystals with the diameter of several tens of nm and the length/diameter ratios of 10 and more. Nanorods are one-dimensional objects with electronic properties and therefore attract an increasingly growing interest towards their applications in novel electronic and optoelectronic devices.[2-4] In case of nanorods, a fine control of growth is necessary because they are extremely sensitive to growth conditions. The physical properties and shape of nanorods are strongly dependent on the growth mechanism. Hence, it is essential to

understand the growth mechanism. So far, there were a lot of studies on the mechanism of nanorods. Some examples are vapor–liquid–solid (VLS),[5, 6] vapor–solid–solid (VSS),[7-9] solid–liquid–solid (SLS),[10] solution–liquid–solid (SLS) growth processes.[11, 12]

### 2.3.1 Vapor-liquid-solid growth mechanism

The typical procedure of the VLS growth of nanorods is shown schematically in Fig. 2.4.[5] First, the catalyst  $B$  (e.g., Au) is deposited onto substrate (e.g., Si), then the substrate is transferred to a growth chamber and annealed before the nanorods are grown. Annealing leads to the formation of drops of liquid alloy  $B$  (e.g., Au) on the substrate. The deposition of material  $A$  from the vapor phase or molecular beam makes the alloy supersaturated. The nanorod grows due to the crystallization of supersaturated alloy on the crystal surface under the drop. This mechanism is so called absorption induced growth mechanism. The higher growth rate of nanorods is explained by a faster chemical reaction or better adsorption on the liquid surface and a faster nucleation of crystal phase from the liquid drop.

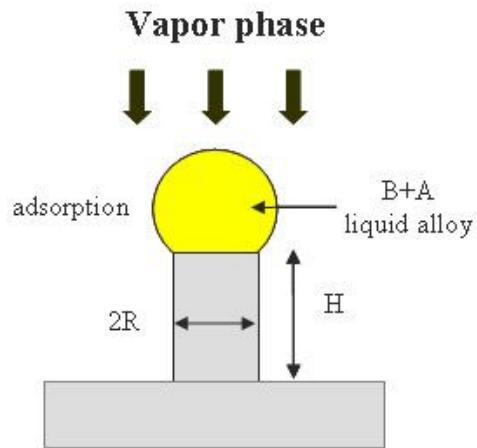
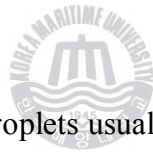


Fig. 2.4 Nanorod of material  $A$  of radius  $R$  and height  $H$  grown on the substrate activated by the drops of liquid alloy  $B+A$ .



Since the initial eutectic droplets usually have a broad size distribution and the nanorods lateral size is usually of order of the size of drop, the lateral size dependence of the normal growth rate of nanorods has been studied experimentally in many systems.[13-15] From this mechanism, nanorod length  $L$  normally increases with their diameter  $D$ ; thus thicker nanorods grow faster than thinner ones. For very thick nanorods, the growth rate is determined by the balance of adsorption and desorption processes on the planar surface of liquid alloy.

### 2.3.2 Vapor-solid-solid growth mechanism

The vapor-solid-solid (VSS) process is a conventional growth mechanism used for interpreting the growth of nanostructure. In this process, the vapor species are first generated by evaporation, chemical reduction, and other kinds of gaseous reactions. These species are subsequently transported and condensed onto the surface of a solid substrate placed in a zone with temperature lower than that of the source material. With control over the supersaturation factor, one could easily obtain one-dimension (1D) nanostructures. As an example, T.I. Kamins et al. reported on Ti-catalyzed Si nanowires by CVD.[8] Many metal-catalyzed Si nanowires were grown by the traditional VLS process, with a metal-containing liquid nanoparticle moving along with the tip of the wire. Although Ti-catalyzed Si nanowire growth appears similar in many ways, the details of the growth mechanism are likely to be different. The catalytic reaction forms a very thin, Si-rich layer (a few monolayers) on the surface of the  $\text{TiSi}_2$  particle at the growing end of the wire. The excess Si near the surface results in a concentration gradient that causes the excess Si to diffuse into the  $\text{TiSi}_2$  island. The excess Si is likely to precipitate, usually at a surface or at an interface. To form macroscopic quantities

of Si on the free surface of the  $\text{TiSi}_2$ , an additional interface must be formed, probably increasing the energy of the system. On the other hand, if the excess Si diffuses to the underlying  $\text{TiSi}_2/\text{Si}$  interface, it can attach to the Si there without requiring an additional interface, and the energy of the system does not need to increase. As the Si atoms precipitate on the underlying Si, the  $\text{TiSi}_2$  island is pushed up, forming a wire.

The above arguments suggest that the  $\text{TiSi}_2$  can move along with the growing wire tip, creating a Si wire with no  $\text{TiSi}_2$  at the base. Therefore, the growth process—especially analogies to the VLS technique—should be considered in more detail. The VLS technique relies on an intermediate, liquid, metal–Si nanoparticle between the incoming vapor and the growing Si wire. The growth temperature is higher than a metal–Si eutectic temperature reported on the binary phase diagram (possibly reduced somewhat because of the small size of the particle).[16] However, the lowest liquid eutectic shown on the published binary phase diagram for Ti and Si is above 1300 °C, while the wires of primary interest in this study were grown in the mid-600 °C temperature range. Even if the eutectic temperature is reduced by the small size of the particle, it is unlikely to reach the

600 °C temperature range.[16] Thus, it is likely that tip growth of Ti-catalyzed Si nanowires occurs by a process analogous to the traditional VLS mechanism, with the catalyzing nanoparticle remaining in the solid phase, rather than being in the liquid phase.

### 2.3.3 Solid-liquid-solid growth mechanism

This mechanism is similar to VLS mechanism. In this process, the only possible source comes from the bulk substrate because no extra source was introduced into the vapor phase. First, deposited metal thin layer forms eutectic liquid alloy droplets with substrate. Because of the relatively high solubility of droplets, more source atoms will diffuse through the solid (substrate)–liquid interface into the liquid phase. A second liquid–solid (nanorod) interface will form when the liquid phase becomes supersaturated due to thermal or compositional fluctuations, resulting in the growth of nanorods. Because this growth process involves solid–liquid–solid phases, it is called SLS growth which is, in fact, an analogous to the VLS mechanism. The growth process of a-Si nanorods via an SLS model is depicted schematically in Fig. 2.5.[10]



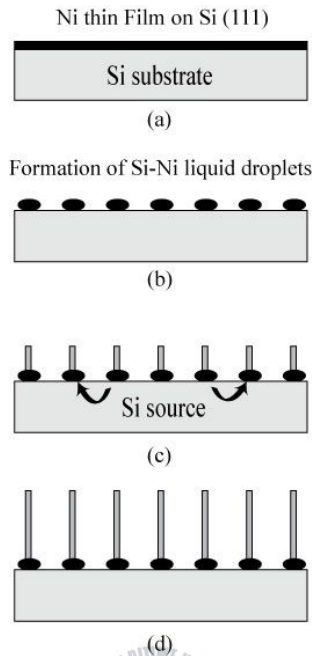


Fig. 2.5. Schematic depiction of Si nanorods growth by the SLS mechanism: (a) deposition of a thin layer of Ni on the Si(111) substrate; (b) formation of the Si–Ni eutectic liquid droplets; (c) continuous diffusion of Si atoms through the substrate–liquid (SL) interface into the liquid droplets, and growth of Si nanorods through the liquid–wire (LS) interface; (d) final state of Si nanorod growth. The smooth surface of the original substrate becomes rough at the end of Si nanorod growth.[10]

### 2.3.4 Diffusion induced growth

Since VPT growth method always proceeds at higher supersaturations of

gaseous phase, it may provide an opportunity to achieve larger  $L/D$  ratios at smaller diameters  $D$ . However, the mechanism of nanorod formation during VPT remains in largest measure unformulated. In contrast to the majority of CVD techniques of nanorod formation, in VPT growth the nonactivated surface may grow with the rate comparable to the deposition rate. Here the question arises: if the maximum growth rate of nanorods is limited by the deposition rate, why is their length much higher than the nominal thickness of deposited material? In contrast to CVD, the VPT growth implies very high values of the diffusion length of adsorbed atoms (adatoms)  $\sim 1\text{--}10\ \mu\text{m}$ , which is of order or higher than the typical whisker lengths. Therefore, the contribution of the adatom diffusion into the overall growth behavior of nanorods should be carefully investigated. An important step in studying the mechanisms of nanorod formation during MBE was taken by Schubert *et al.*, [17] who reported the  $L(D)$  dependence of Si whiskers grown on the Si(111)-Au surface. Expecting the usual VLS growth to proceed, the authors found that narrower whiskers grew much faster than the thicker ones. The measured  $L(D)$  dependence was found to be close to the inversely proportional relation  $L \sim A/D$ . Such form of  $L(D)$  dependence is typical for the diffusion induced (DI) growth of wire like

crystals that was investigated theoretically and experimentally by Sears [18, 19] and Dittmar and Neumann.[20, 21] DI growth is controlled by the diffusion of adatoms towards the nanorod top along their side facets. When the surface is activated by the growth catalyst, the drop of a liquid alloy on the top of nanorod may be quite an attractor for the adatoms and VLS growth may take many features of the DI one. Technologically it is important that VPTC technique may enable growing nanorods whose length is much higher than the effective thickness of deposited material (when the DI mechanism dominates), because the growth rate of nanorods in the DI mode is no longer restricted by the deposition rate.

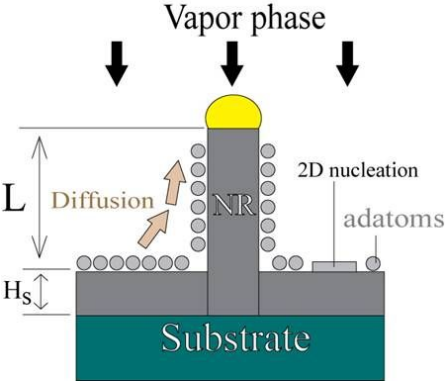


Fig. 2.6. The model of nanorod growth during VPT. Nanorod is assumed as being a cylinder of diameter  $D=2R$  and length  $L$ , the contact angle of drop is assumed to be  $90^\circ$ .

The growth mechanism of one-dimensional nanostructures has been well explained by V.G. Dubrovskii et al,[5, 6] and it is worthy to look over the fundamentals of their explanation. They assume that the atoms may arrive into the drop not only from the source but also from the substrate surface due to diffusion along the side facets of NRs. Theoretical expression on this model was developed as follows.[5, 6] In steady state the normal growth rate of NR  $dL/ dt$  is given by

$$\frac{\pi R^2}{\Omega} \frac{dL}{dt} = \left( \frac{V - V_s}{\Omega} - \frac{2Cr_l}{\tau_l} \right) \pi R^2 + j_L \quad (1)$$

Here  $L(t)$  is the NR length at time  $t$  measured from the surface of the epitaxial layer, growing on the substrate surface and having the thickness of  $H_s(t)$ ,  $R$  is the NR radius,  $V_s$  is the growth rate of nonactivated surface,  $V$  is the deposition rate,  $\Omega$  is the volume per atom in the crystal,  $C$  is the volume concentration of alloy,  $r_l$  is the interatomic distance in the liquid phase,  $\tau_l$  is the mean lifetime of atoms in the liquid, and  $j_L$  is the diffusion flux of adatoms towards the top of NR. The first term in Eq. (1) stands for absorption on the liquid surface, the second for desorption, and the third describes the diffusion induced (DI) contribution to the growth rate.

In many experimental cases, this equation is reduced to

$$L = \left( c + \frac{D^*}{D} \right) H, \quad (2)$$

where  $H$  is the effective thickness ( $H=Vt$ ),  $D^*$  is characteristic diameter at which the DI effects become predominant. And  $c$  is constant related to absorption and desorption rate.



## REFERENCES

- [1] Guozhong Cao, *Nanostructures & nanomaterials*, Imperial College Press (2004).
- [2] C.L. Hsin, J.H. He, and L.J. Chen, *Appl. Phys. Lett.* 88, 063111 (2006).
- [3] Y.J. Li, M.Y. Lu, C.W. Wang, K.M. Li, and L.J. Chen, *Appl. Phys. Lett.* 88, 143102 (2006).
- [4] J. Zhong, S. Muthukumar, Y. Chen, Y. Lu, H.M. Ng, W. Jiang and E.L. Garfunkel, *Appl. Phys. Lett.* 83, 3401 (2003).
- [5] V.G. Dubrovskii and N.V. Sibirev, *Phys. Rev. E* 70, 031604 (2004).
- [6] V.G. Dubrovskii, G.E. Cirlin, I.P. Soshnikov, A.A. Tonkikh, N.V. Sibirev, Y.B. Samsonenko, and V.M. Ustinov, *Phys. Rev. B* 71, 205325 (2005).
- [7] G.A. Bootsma, and H.J. Gassen, *J. Cryst. Growth* 10, 223 (1971).
- [8] T.I. Kamins, R.S. Williams, D.P. Basile, T. Hesjedal, and J.S. Harris, *J. Appl. Phys.* 89, 1008 (2001).
- [9] A.I. Persson, M.W. Larsson, S. Stenstroöm, B.J. Ohlsson, L. Samuelson, and L.R. Wallenberg, *Nat. Mater.* 3, 677 (2004).

- [10] a) D.P. Yu, Y.J. Xing, Q.L. Hang, H.F. Yan, J. Xu, Z.H. Xi, and S.Q. Feng, *Phys. E* 9, 305 (2001). b) A. Gorbunov, O. Jost, W. Pompe, and A. Graff, *Carbon* 40, 113 (2002). c) H.F. Yan, Y.J. Xing, Q.L. Hang, D.P. Yu, Y.P. Wang, J. Xu, Z.H. Xi, and S.Q. Feng, *Chem. Phys. Lett.* 323, 224 (2000).
- [11] a) T.J. Trentler, K.M. Hickman, S.C. Goel, A.M. Viano, P.C. Gibbons, and W.E. Buhro, *Science* 270, 1791 (1995). b) Y.P. Fang, X.G. Wen, S.H. Yang, and *Angew. Chem. Int. Ed.* 45, 4655 (2006).
- [12] F.M. Davidson, D.C. Lee, D.D. Fanfair, and B.A. Korgel, *J. Phys. Chem. C.* 111, 2929 (2007).
- [13] *Handbook of Crystal Growth*, edited by D. T. J. Hurle (Elsevier, Amsterdam, 1994), Vol. 2.
- [14] K. Hiruma, M. Yazawa, T. Katsuyama, K. Ogawa, K. Haraguchi, M. Koguchi, and H. Kakibayashi, *J. Appl. Phys.* 77, 447 (1995).
- [15] E.I. Givargizov, *J. Cryst. Growth* 20, 217 (1973).
- [16] M. Wautelet, J.P. Dauchot, and M. Herq, *Nanotechnology* 11, 6 (2000).
- [17] L. Schubert, P. Werner, N. D. Zakharov, G. Gerth, F.M. Kolb, L. Long, U. Gösele, and T.Y. Tan, *Appl. Phys. Lett.* 84, 4968 (2004).



[18] G.W. Sears, *Acta Metall.* 1, 457 (1953).

[19] G.W. Sears, *Acta Metall.* 3, 367 (1955).

[20] W. Dittmar and K. Neumann, in *Growth and Perfection of Crystals*, edited by  
R. H. Doremus, B. W. Roberts, and D. Turnbull (Wiley, New York, 1958).

[21] W. Dittmar and K. Neumann, *Z. Elektrochem.* 64, 297 (1960).





# Chapter 3. Growth mechanism of ZnO nanorods on various catalysts

## 3.1 Introduction

Nanostructures exhibit peculiar and fascinating properties compared with their bulk counterparts. In nanostructures, the density of states of carriers is concentrated to a certain levels of energy, which enables enhancement of exciton oscillator strength and light-emitting efficiency. As a result, the performance of nanostructure-based optical devices is expected to be improved and to be less temperature dependent.[1]

One-dimensional (1D) nanostructure materials, such as nanotubes, nanowires and nanobelts have attracted much attention because of their interesting properties for understanding fundamental physical concepts and for portential applications [2-6]. Among the wide variety of 1D semiconductor nanostructures, ZnO nanorods attract special interest for optoelectronic nano-devices due to the simple structural configuration. In the last few years, several methods have been employed to synthesize 1D ZnO nanostructures.[7-10] Particularly, catalysts have

been often used for the growth of nanorods (Table 3.1).

Table 3.1. Various catalysts and growth methods of ZnO nanorods

Catalysts	Substrates	Growth methods	References
Au	Si	Electrochemical deposition	[11]
	SiO <sub>2</sub>	Physical vapor deposition	[12]
	4H-SiC	Inductive heating	[13]
	Al <sub>2</sub> O <sub>3</sub>	Physical vapor deposition	[14]
		Vapor phase transportation	[15]
AuGe	Si	Vapor phase transportation	[16, 17]
Ag	Si	Vapor phase transportation	[16]
	SiO <sub>2</sub> , SiN <sub>x</sub>	Molecular beam epitaxy	[18]
Ti	Si	Vapor phase transportation	[16]
AuTi	Si	Metal organic chemical vapor deposition	[19]
Al	Si	Vapor phase transportation	[16]

However, it has been seldom studied on the effect of catalysts on growth

mechanism. In order to control potential properties of nanorods, a clear understanding on growth mechanism of nanorods is more required yet.

In this chapter, it is reported on the growth of well-aligned 1D ZnO nanorods on AuGe and Ti as catalysts by VPT method. ZnO nanorods are investigated theoretically and experimentally. The effects from catalysts on the growth mechanism have been investigated in terms of variation of surface energy.

### 3.2 Experimental details

The growth temperature determines the vapor pressure of Zn and thermodynamic processes. It should be pointed out that if the ambient temperature of this process is too high, oxygen vaporization will be accelerated and the nanostructure tends to contain a lot of oxygen deficiencies. Various reports support this description, generally at high growth temperature the degradation of optical property and lose uniformity are observed.[20] Generally VPT growth system using in this study is able to synthesize ZnO nanorods at the growth temperature from 600 to 650 °C. First, two substrates were prepared. AuGe and Ti (thickness~50nm) metals were deposited on Si(111) substrates. Zn source (4N purity, powder-type)

and each substrate were loaded in a quartz tray, which has two parts; one (lower part of tray) is for loading source, the other (upper part) is for substrate. The evaporated Zn vapor is designed to be supplied on to the substrates through via hole in the upper part of tray. When the horizontal quartz tube furnace reached to growth temperature the quartz tray was inserted into the quartz tube furnace for the nanorods growth. The growth temperature was 650 °C. After 30 min. growth, quartz tray was ejected out into air and cooled down quickly. Finally, ZnO nanorods on each substrate under different catalysts were obtained. Dry N<sub>2</sub> was used as a carrier gas, and flows through the quartz tube during the growth with the flow rate of 500 (ml/min). The surface morphology of each sample was observed by the Quanta 200 FEG scanning electron microscope (SEM) with a field emission gun, operation in the regime of secondary electron emission.

### **3.3 Characterization of ZnO nanorods on various catalysts**

Conventional growth model explains the growth mechanism of 1D nanostructure involving the participation of VLS in the growth process. During the growth process, the catalyst absorbs the vapor components such as Zn (vapor) and

$Zn_xO$  ( $x < 1$ , vapor), to form a eutectic alloy. When it is supersaturated, crystallization of ZnO will occur.[21] The catalysts play an important role of formation of eutectic alloy.

In this experiment, AuGe and Ti catalysts were deposited by thermal evaporator and e-beam evaporator on Si substrates. From the phase diagram of AuGe,[22] the eutectic melting point of it ( $Au_{1-x}Ge_x$ ;  $x \sim 43$  at. %) is estimated to be 560 °C and the melting point of Ti is 1668 °C. One play role of catalyst in liquid state and the other one play role of catalyst in solid state during the ZnO nanorods growth.



Fig. 3.1 shows the respective SEM images for (a) ZnO nanorods/Ti, and (b) ZnO nanorods/AuGe. Also the insets show plain view images for each sample. The ZnO nanorods were successfully obtained through two catalysts. For ZnO nanorods grown on Ti, the minimum diameter is about 32 nm and the maximum is about 110 nm. The length of nanorods amounts to 2961 nm at  $D=32$  nm and decreases to 1539 nm at  $D=110$  nm, the  $L/D$  ratio thus changing from 93 for the thinnest nanorods down to 14 for the thickest ones.

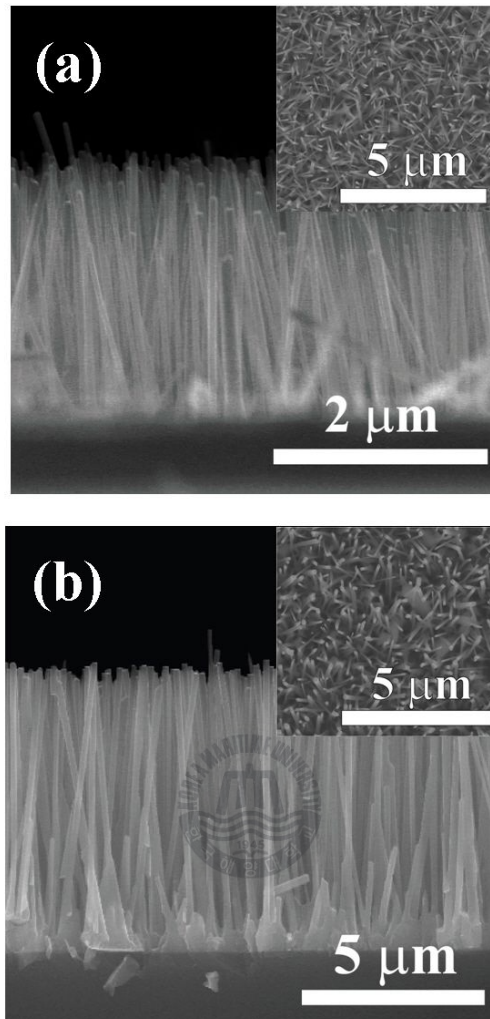


Fig. 3.1. Cross-sectional SEM images of ZnO nanorods on various catalysts, the insets are plain-view image. (a) ZnO nanorods/Ti, and (c) ZnO nanorods/AuGe.

On the other hands, for ZnO nanorods on AuGe, the minimum diameter  $D$  is about 61 nm and the maximum is about 208 nm. The length of nanorods is  $L=7000$  nm at  $D=61$  nm also it decreases to  $L=2345$  nm at  $D=208$  nm, the  $L/D$

ratio thus changing from 114.75 for the thinnest nanorods down to 11.27 for the thickest ones.

Note that, it is hard to transform Ti metal into liquid phase due to a high melting point of it. According to previous study, low-temperature growth of ZnO nanorods from solid catalysts as being an intermediate between the VLS and VS processes [23]. It is not necessary to form droplets in liquid state as a catalyst during the process. It is likely that the growth of nanorods occurs by a process analogous to the traditional VLS mechanism, with the catalyzing nanoparticle remaining in the solid phase, rather than being in the liquid phase.[24] On the basis of these observations, I propose that the growth of ZnO nanorods is affected not the state of catalyst but the kind of catalyst.

### **3.4 The effect of catalyst on the growth of ZnO nanorods**

From the analysis of SEM images, it is obtained the experimental length to diameter  $L(D)$  dependencies of nanorods as shown in Fig. 3.2. From  $L(D)$  curves it is seen that the length of nanorods decreases with their diameter for two samples. For the usual explanation of nanorods growth mechanism, the lateral size

dependence of the normal growth rate of nanorods has been studied experimentally in many systems.[25-27] In the VLS mechanism, nanorods are assumed to grow due to the adsorption and solidification of vaporized atoms from the drop surface. The higher growth rate of nanorods in the VLS mechanism is explained by a faster chemical reaction or an increase in adsorption on the liquid drop surface. Therefore, the nanorod length  $L$  normally increases with their diameter  $D$ . Note that it is clearly opposite to the observation in this study.

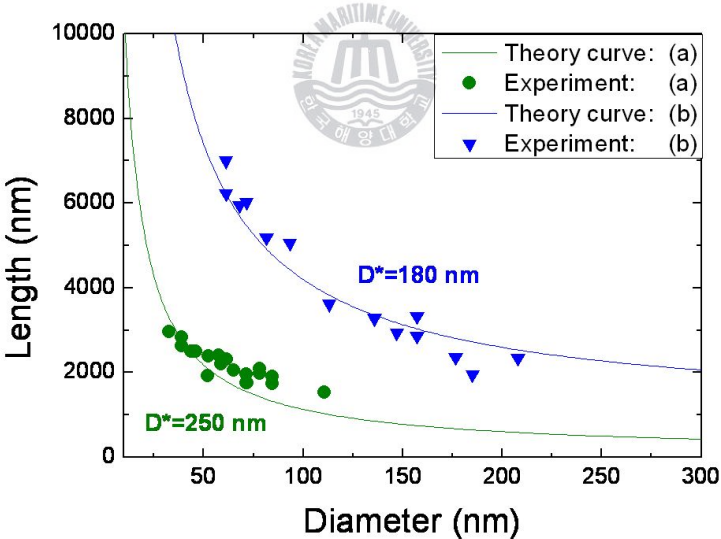


Fig. 3.2. Experimental and theoretical length/diameter dependencies for (a) ZnO nanorods on Ti, (b) ZnO nanorods on AuGe. The theoretical curves are obtained from Eq. (2) in chapter 2.



As shown in the Fig. 3.2, the measured  $L(D)$  dependence was an inversely proportional relation  $L \sim (A/D)$ . Such form of  $L(D)$  dependence has been attributed to a diffusion induced growth (DI growth) and mainly reported from molecular beam epitaxy and chemical vapor deposition of whiskers.[28, 29]

Theoretical  $L(D)$  dependency curves given by Eq. (2) in the chapter 2 are presented in the same figures (Fig. 3.2). The curves show larger characteristic diameter  $D^*$  on Ti than that on AuGe. The fact means that ZnO nanorods on Ti have longer effective diffusion length of adatoms than that on AuGe. For DI growth mechanism, surface energy of catalyst is very important to diffusion length of adatoms. The diffusion length on the surface is limited by desorption and is given by [30]

$$\lambda_s = \lambda \exp[(\Delta G_{dep} - \Delta G_s) / 2kT] \quad (1)$$

where,  $\Delta G_{dep}$  is binding energy of the adatom to the surface.  $\Delta G_s$  is the activation energy for surface diffusion. Note that, the binding energy of the adatom to the surface gives more effects to variation of diffusion length than the activation energy for surface diffusion. On the one hand, the binding energy is deeply related to surface energy. The surface energy of Ti ( $S_{Ti}$ ) is higher than  $S_{Si}$  and  $S_{AuGe}$  under

growth temperature ( $S_{Ti} \sim 1900$  ergs/cm<sup>2</sup>,  $S_{Si} \sim 800$  ergs/cm<sup>2</sup>,  $S_{AuGe} \sim 730$  ergs/cm<sup>2</sup> in APENDIX). Therefore, Ti catalyst gives larger effective diffusion length of adatoms on surface than AuGe or Si as shown Fig. 3.2.

### 3.5 Conclusion

It has been shown that the measured  $L(D)$  dependence is an inversely proportional relation  $L \sim (A/D)$ . Experimental results show a considerable agreement with theoretical  $L(D)$  curves. The curves show larger characteristic diameter  $D^*$  on Ti than that on AuGe. The fact indicates that ZnO nanorods on Ti show longer diffusion length of adatoms than that on AuGe. It is related to the surface energy of catalysts deeply. Ti has larger surface energy under growth temperature 650 °C than AuGe and Si. Thus, VPT growth of ZnO nanorods can be explained in terms of VLS mode by DI growth model in that the surface energy of catalyst is very important to control growth of nanorods in that variation of adatom's diffusion length.

## REFERENCES

- [1] Y. Arakawa and H. Sasaki, *Appl. Phys. Lett.* 40, 2152 (1982).
- [2] Y.J. Xing, Z.H. Xi, and Z.Q. Xue, *Appl. Phys. Lett.* 83, 1689 (2003).
- [3] M.H. Huang, Y. Wu, and H. Feick, N. Tran, E. Weber, and P. Yang, *Adv. Mater.* 13, 113 (2001).
- [4] X.Y. Kong and Z.L. Wang, *Appl. Phys. Lett.* 84, 975 (2004).
- [5] W.L. Hughes and Z.L. Wang, *J. Am. Chem. Soc.* 126, 6703 (2004).
- [6] Z.L. Wang, X.Y. Kong and J.M. Zuo, *Phys. Rev. Lett.* 91, 185502 (2003).
- [7] J.J. Wu and S.C. Liu, *Adv. Mater.* 14, 215 (2002).
- [8] Y.C. Kong, D.P. Yu and B.Zhang, *Appl. Phys. Lett.* 78, 407 (2001).
- [9] C.X. Xu, X.W. Sun, and B.J. Chen, *Chem. Phys. Lett.* 20, 1319 (2003).
- [10] C.X. Xu, X.W. Sung, and B.J. Chen, *J. Appl. Phys.* 95, 661 (2004).
- [11] B. Cao, W. Cai, and H. Zeng, *Appl. Phys. Lett.* 88, 161101 (2006).
- [12] S.R. Hejazi, H.R. Madaah Hosseini, and M. Sasani Ghamsari, *J. Alloy. Comp.* 455, 353 (2008).
- [13] L. Luo, B.D. Sosnowchik, and L. Lin, *Appl. Phys. Lett.* 90, 093101 (2007).

- [14] L.C. Campos, S.H. Dalal, D.L. Baptista, R. Magalhães-Paniago, A.S. Ferlauto, W.I. Milne, L.O. Ladeira, and R.G. Lacerda, *Appl. Phys. Lett.* 90, 181929 (2007).
- [15] X. Wang, C.J. Summers, and Z.L. Wang, *Nano Lett.* 4, 423 (2004).
- [16] M.N. Jung, S.J. Oh, J.E. Koo, S.N. Yi, B.W. Lee, W.J. Lee, D.C. Oh, T. Yao, and J.H. Chang, *Curr. Appl. Phys.* 9, e161 (2009).
- [17] M.N. Jung, J.E. Koo, S.J. Oh, B.W. Lee, W.J. Lee, S.H. Ha, Y.R. Cho, and J.H. Chang, *Appl. Phys. Lett.* 94, 041906 (2009).
- [18] L.C. Tien, D.P. Norton, S.J. Pearton, Hung-Ta Wang, and F. Ren, *Appl. Surf. Sci.* 253, 4620 (2007).
- [19] C.J. Park, D.K. Choi, J.K. Yoo, G.C. Yi, and C.J. Lee, *Appl. Phys. Lett.* 90, 083107 (2007).
- [20] C. Andreazza, P. Andreazza and D. Zhao, *Superlatt. and Microstruct.* 39, 340 (2006).
- [21] E. McGlynn, J. Grabowska, and K.K. Nanda, *Sur. & Coat. Tech.* 20, 1093 (2005).
- [22] Okamoto, H., Massalski, T.B.: *Bull. Alloy Phase Diagrams* 5 (1984) 601

- [23] L.C. Campos, M. tonezzer, A.S. Ferlauto, V. Grillo, R.M. Paniago, S. Oliveira, L.O. Ladeira, and R. G. Lacerda, *Adv. Mater.* 20, 1499 (2008).
- [24] T.I. Kamins, R.S. Williams, D.P. Basile, T. Hesjedal, and J.S. Harris, *J. Appl. Phys.* 89, 1008 (2001).
- [25] *Handbook of Crystal Growth*, edited by D. T. J. Hurle (Elsevier, Amsterdam, 1994), Vol. 2.
- [26] K. Hiruma, M. Yazawa, T. Katsuyama, K. Ogawa, K. Haraguchi, M. Koguchi, and H. Kakibayashi, *J. Appl. Phys.* 77, 447 (1995).
- [27] E.I. Givargizov, *J. Cryst. Growth* 20, 217 (1973).
- [28] W. Dittmar and K. Neumann, in *Growth and Perfection of Crystals*, edited by R. H. Doremus, B. W. Roberts, and D. Turnbull (Wiley, New York, 1958).
- [29] W. Dittmar and K. Neumann, *Z. Elektrochem.* 64, 297 (1960).
- [30] K.N. Ti, J.W. Mayer, and L.C. Feldman, «Electronic Thin Film Science for electrical engineers and materials scientists», Macmillan Publishing Company, a division of Macmillan, Inc. (1992).

# Chapter 4. Growth mechanism of Impurity doped ZnO nanorods

## 4.1 Introduction

ZnO has been known as an important II-VI semiconductor with wide direct band gap of 3.37eV at RT, and large exciton binding energy of 60meV.[1] And also, ZnO nanorods have the simple structural configuration. So they attract special interest for optoelectronic nano-devices. For examples, optically pumped ultraviolet lasing from the vertically grown ZnO nanorods was demonstrated at room temperature by Huang et al.[2] And then Johnson et al.[3, 4] investigated more detailed lasing properties from the single ZnO nanorod using a high resolution optical microscope. They suggested that the spontaneous and stimulated emissions were closely related to the waveguides behaviors. It was estimated, from the fractional mode power of cylindrical waveguide mode, that the field intensity over 90% was retained in the nanorod with the diameter above 200 nm, while the field intensity less than 25% was remained inside the wire with the diameter of 100 nm. The possibility applications of the ZnO nanorods was considered as electric,

optical, energy conversion and sensing devices such as field emitter,[5] field-effect transistor (FET),[6-8] light emitting diode (LED),[9] dye-sensitized solar cell,[10] and sensor.[11-13] For those applications, conductivity control by impurity doping is inevitable. Also in the last few years, many researches have been performed on the doping of ZnO nanorods (Table 4.1).

Table 4.1. Various dopants of ZnO nanorods

Dopants	Substrate	Growth method	References
Al	Si	Thermal evaporation	[14-16]
Mn	ZnO	Chemical vapor deposition	[17]
Sn	Si	Thermal evaporation	[18]
Ga	Si	Vapor phase transportation	[19]
In	Si	Thermal evaporation	[20]
		Vapor phase transportation	[21]

In this chapter, I will describe on the growth mechanism of In-doped ZnO nanorods by using VPT method. The aim of this work is theoretical and

experimental investigation of the growth mechanism of ZnO:In nanorods. A diffusion-induced kinetic model of ZnO nanorods growth will be presented that describes the adatom diffusion from the surface of epitaxially growing layer to the nanorod top. As increasing In contents, the effective vapor pressure of adatom will be changed and lead an variation of effective diffusion length.

## 4.2 Experimental details

ZnO:In nanorods were grown by vertical vapor phase transportation (V-VPT) method on various substrates. The apparatus design is same in chapter 3. First of all, AuGe was deposited on Si(111) substrates as a catalyst. To control the In composition, Zn mixed In powder sources (Weight ratio; In/(In+Zn): 0, 0.8, 0.16) and each substrate were loaded in a quartz tray. When the horizontal quartz tube furnace reached to growth temperature the quartz tray was inserted into the quartz tube furnace for the nanorods growth. The growth temperature was 600 °C. After growth, quartz tray was ejected out into air and cooled down quickly. ZnO:In nanorods with different In composition were obtained. Dry Ar was used as a carrier gas, and flows through the quartz tube during the growth with the flow rate of 600



(ml/min). It was used EDX measurement to investigate In distribution in ZnO:In nanorods. The surface morphology of each sample was observed by the Quanta 200 FEG scanning electron microscope (SEM) with a field emission gun, operation in the regime of secondary electron emission.

### 4.3 Characterization of In doped ZnO nanorods

Conductivity control of nanocrystals including nanorods is not so simple and has several fundamental difficulties; the typical doping concentration of  $10^{18} \text{ cm}^{-3}$  means just one dopant atom in  $10 \text{ nm}^3$ , thus any distribution fluctuation of dopant will result in a totally different functionality of device. Making the further complicated situation is the distribution of the dopant atoms. Certainly surface atom would behave differently from the centered atom. To meet such a challenge, the ability of manipulating the growth process is crucial, but it has not been considered seriously yet. In this experiment, ZnO:In nanorods by simple vertical vapor phase transportation method were synthesized.

Fig. 4.1 shows the respective SEM images for ZnO:In nanorods/AuGe with different In composition. Also the insets show plain view images for each

sample. The In composition of sample is characterized by energy dispersive x-ray (EDX) spectroscopy.

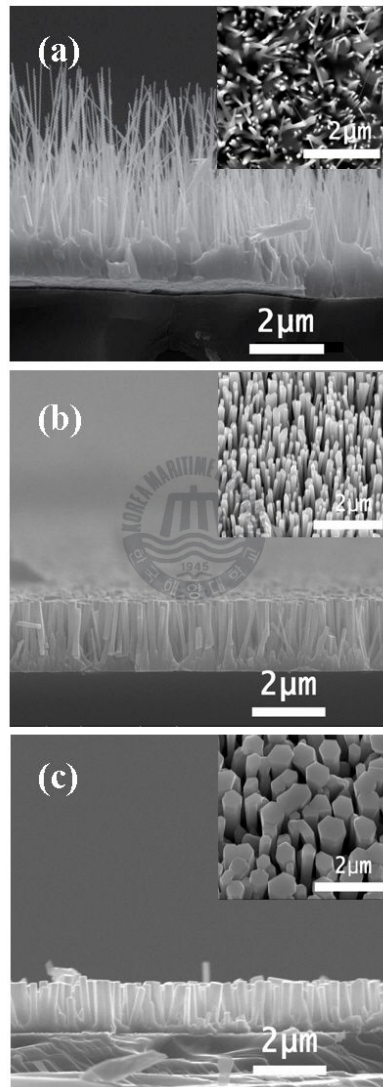


Fig. 4.1. Cross-sectional SEM images of ZnO:In nanorods/AuGe with different In composition, the insets are plain-view image. (a) pure ZnO nanorods, (b) ZnO:In<sub>0.27</sub> nanorods and (c) ZnO:In<sub>0.33</sub> nanorods.

For pure ZnO nanorods (without any In contents), the minimum diameter is about 70 nm and the maximum is about 85 nm. The length of nanorods amounts to 4670 nm at  $D=70$  nm and decreases to 4295 nm at  $D=85$  nm, the  $L/D$  ratio thus changing from 67 for the thinnest nanorods down to 51 for the thickest ones. For ZnO:In<sub>0.27</sub> nanorods, the minimum diameter  $D$  is about 94 nm and the maximum is about 170 nm. The length of nanorods is  $L=1539$  nm at  $D=94$  nm also it decreases to  $L=1127$  nm at  $D=170$  nm, the  $L/D$  ratio thus changing from 16 for the thinnest nanorods down to 7 for the thickest ones. For ZnO:In<sub>0.33</sub> nanorods, the minimum diameter  $D$  is about 140 nm and the maximum is about 300 nm. The length of nanorods is  $L=1038$  nm at  $D=140$  nm also it decreases to  $L=736$  nm at  $D=300$  nm, the  $L/D$  ratio thus changing from 7 for the thinnest nanorods down to 2.5 for the thickest ones.

The nanorod length  $L$  clearly decreases with increasing their diameter  $D$  and In composition. Such form of  $L(D)$  dependence has been attributed to DI growth. Although DI growth of nanorods with additional impurity atoms has not been studied yet, it may have large influence on the nanorod growth since impurity atoms generally have different sticking coefficients and migration lengths in

comparison with the host atoms.[21]

#### 4.4 The effect of dopants on the growth of ZnO nanorods

The growth system in this study is agreed with DI growth mechanism. The most important factor distinguished the DI growth from VLS mechanism may be the fact that DI growth is controlled by the diffusion of adatoms toward the nanorod top along their side facets. Therefore the variation of adatom's vapor pressure will leads more complex growth process.

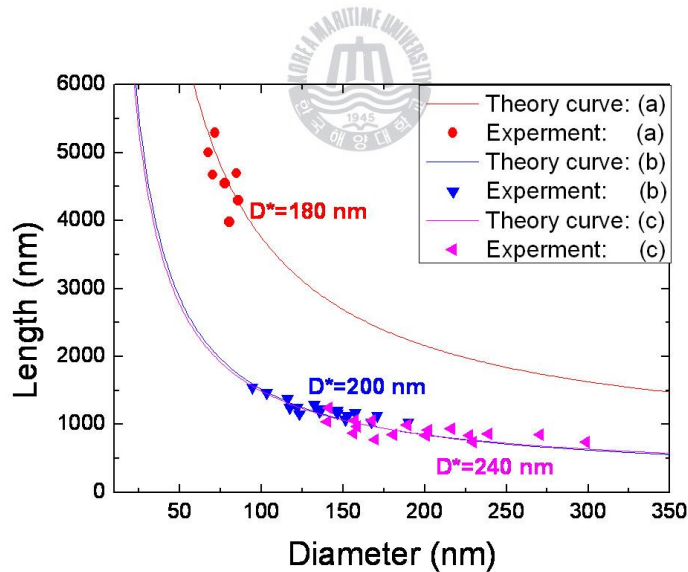


Fig. 4.2. Experimental and theoretical length/diameter dependencies for (a) pure ZnO nanorods, (b) ZnO:In<sub>0.27</sub> nanorods and (c) ZnO:In<sub>0.33</sub> nanorods. The theoretical curves are obtained from Eq. (2) in chapter 2.

From the analysis of SEM images, the experimental  $L(D)$  dependencies of nanorods are plotted with theoretical  $L(D)$  dependency curves in Fig. 4.2. It indicates that each sample has different characteristic diameter  $D^*$ . The characteristic diameter  $D^*$  increased with increasing In content. Major factors related to the  $D^*$  are effective diffusion length of adatom. Adatom's diffusion length is related to binding energy of adatom to the surface  $\Delta G_{dep}$ . It means the energy needed to remove it from the surface to the vapor. Since In atoms have lower vapor pressure than Zn atoms, the characteristic diameter  $D^*$  would be increased with increasing In composition, simply because it is directly related to the number of deposited particles in the surface.


## 4.5 Conclusion

ZnO:In nanorods by simple vertical vapor phase transportation method were synthesized. Each sample has different characteristic diameter  $D^*$ . The characteristic diameter  $D^*$  increased with increasing In content. Adatom's diffusion length is related to the energy needed to remove it from the surface to the vapor. Since In atoms have lower vapor pressure than Zn atoms, the characteristic

diameter  $D^*$  would be increased with increasing In composition, simply because it is directly related to the number of deposited particles in the surface. Thus, dopants affect vapor pressure of adatom and lead the variation of their diffusion length.



## REFERENCES

- [1] D.C. Reynolds, D.C. Look, B. Jogai et al, *J. Appl. Phys.* 88, 2152 (2002).
- [2] M.H. Huang, S. Mao, H. Feick, H. Yan, Y. Wu, H. Kind, E. Weber, R. Russo, and P. Yang, *Science* 292, 1897 (2001).
- [3] J.C. Johnson, H. Yan, R.D. Schaller, L.H. Haber, R.J. Saykally, and P. Yang, *J. Phys. Chem. B* 105, 11387 (2001).
- [4] J.C. Johnson, H. Yan, P. Yang, and R.J. Saykally, *J. Phys. Chem. B* 107, 8816 (2003).
- 
- [5] S.H. Jo, D. Banerjee, and Z.F. Ren, *Appl. Phys. Lett.* 85, 1407 (2004).
- [6] H.T. Ng, J. Han, T. Yamada, P. Nguyen, Y.P. Chen, and M. Meyyappan, *Nano. Lett.* 4, 1247 (2004).
- [7] W.I. Park, J.S. Kim, G.C. Yi, M.H. Bae, and H.J. Lee, *Appl. Phys. Lett.* 85, 5052 (2004).
- [8] Z. Fan, and J.G. Lu, *Appl. Phys. Lett.* 86, 032111 (2005).
- [9] R. Konenkamp, R.C. Word, and C. Schlegel, *Appl. Phys. Lett.* 85, 6004 (2004).
- [10] M. Law, L.E. Greene, J.C. Johnson, R. Saykally, and P. Yang, *Nat. Mater.* 4,

455 (2005).

[11] H. Kind, H. Yan, B. Messer, M. Law, and P. Yang, *Adv. Mater.* 14, 158 (2002).

[12] Q. Wan, Q.H. Li, Y.J. Chen, and T.H. Wang, X.L. He, J.P. Li, and C.L. Lin, *Appl. Phys. Lett.* 84, 3654 (2004).

[13] H. T. Wang, B.S. Kang, F. Ren, L.C. Tien, P.W. Sadik, D.P. Norton, S.J. Pearton, and J. Lin, *Appl. Phys. Lett.* 86, 243503 (2005).

[14] H.P. Tang, L.P. Zhu, H.P. He, Z.Z. Ye, Y. Zhang, M.J. Zhi, Z.X. Yang, B.H. Zhao, and T.X. Li, *J. Phys. D* 39, 2696 (2006).

[15] H.P. He, H.P. Tang, Z.Z. Ye, L.P. Zhu, B.H. Zhao, L. Wang, and X.H. Li, *Appl. Phys. Lett.* 90, 023104 (2007).

[16] X.Y. Xue, L.M. Li, H.C. Yu, Y.J. Chen, Y.G. Wang, and T.H. Wang, *Appl. Phys. Lett.* 89, 043118 (2006).

[17] J.J. Liu, M.H. Yu, and W.L. Zhou, *Appl. Phys. Lett.* 87, 172505 (2005).

[18] X.Y. Xue, Y.J. Chen, Y.G. Wang, and T.H. Wang, *Appl. Phys. Lett.* 86, 233101 (2005).

[19] C.X. Xu, X.W. Sun, and B.J. Chen, *Appl. Phys. Lett.* 84, 1540 (2004).

[20] S.Y. Bae, H.C. Choi, C.W. Na, and J.H. Park, *Appl. Phys. Lett.* 86, 033102



(2005).

[21] M.N. Jung, J.E. Koo, S.J. Oh, B.W. Lee, W.J. Lee, S.H. Ha, Y.R. Cho, and J.H.

Chang, *Appl. Phys. Lett.* 94, 041906 (2009).



## Chapter 5. Conclusion

Nanomaterials are being started to be used as a key component for many devices. A versatile chemical and physical property of semiconductor nanostructures depending on their dimensionality, size, and surface area makes the nanomaterials be greatly potential building blocks for electronic, photonic, and sensing device fabrications. So far, a large number of publications have appeared lately reporting nanostructures of various shapes including nanobelts, nanorings, nanotubes, nanopropellers, nanotetrapods, and nanorods grown by spontaneous growth under different growth condition. Since a discovery of carbon nanotubes (CNT) in 1991, 1D nanomaterials have attracted a high interest for years by the merits of their fascinating mechanical, electrical, optical and magnetic properties. Among the wide variety of 1D semiconductor nanostructures, ZnO nanorods have received many attentions for optoelectronic nano-devices and sensing devices due to the simplest structural configuration. Although many studies on ZnO-based nanostructures have been reported, a clear understanding on growth mechanism of nanorods is more required yet. In order to realize fully commercialized devices

based on ZnO nanorods, more detailed investigation on the growth behaviors is highly needed.

In this study, I have grown the vertically well-aligned ZnO nanorods by using simple vertical vapor phase transportation (V-VPT) method. Vapor phase transport (VPT) method is the simplest and widely used method, which provides unique advantage that is the controllability of nanostructure. And I have investigated the growth mechanisms of ZnO nanorods grown with several kinds of catalysts and In dopants by VPT process. In the chapter 2, previous studies on growth mechanisms of nanorods were reviewed. The VPT growth system in this study was clearly opposite to usual explanation of VLS growth process. The growth system is agreed with DI growth mechanism. In the chapter 3, the effects of catalysts on the growth mechanism has been investigated. The length-diameter (L-D) curves for those nanorods show different characteristic diameter  $D^*$  on each catalysts, because the surface energy of catalyst plays an important role to determine the diffusion length of adatoms. And also the growth mechanism of impurity doped ZnO nanorods was focused in the chapter 4. The characteristic diameter  $D^*$  increased with increasing In content. Since dopant affects the vapor

pressure of adatom, it leads the variation of diffusion length of adatom. The achievements in this study are believed to be valuable for further researches on the improved controllable growth of 1D nanostructures.



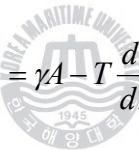
## APPENDIX

### Magnitudes of Surface Energies

The magnitude of the surface tension (or surface energy per unit area) for many materials used in device technology is about 1,000 ergs/cm<sup>2</sup>. From the point of view of thermodynamics, there are two important relations:

$$\frac{d\gamma}{dT} = \frac{-S_s}{A}$$

And


$$E_s = \gamma A - T \frac{d\gamma}{dT} A$$

Where  $S_s$  is the entropy of the surface,  $A$  is the area,  $\gamma$  is the surface tension, and  $T$  is the temperature. These relations allow estimation of the surface tension at room temperature from tabulated value of  $d\gamma/dT$  and measured values of  $\gamma$  taken at the melting temperature. The values of  $d\gamma/dT$  are assumed to be independent of temperature.

To estimate the surface energy for silicon, use Table A.1 to find:

$$\gamma = 730 \text{ erg/cm}^2 \text{ at the melting point}$$

$$\frac{d\gamma}{dT} = -0.1 \text{ ergs/cm}^2/\text{°C}$$

The melting point for silicon  $T_m(\text{Si}) = 1410$  °C. Then at room temperature, the surface energy of silicon is given by

$$\gamma_{RT}(\text{Si}) = 730 + (1410 - 25) \times 0.1 = 869 \text{ ergs/cm}^2$$

The surface energy at the melting point is not very different from the surface energy at temperatures of interest. The small change of the surface energy is associated with the entropy contribution, which is small.

Table A.1. Surface Tension of Liquid Metals [1]

Metal	$\gamma_{LV}$ (ergs/cm <sup>2</sup> )	$\gamma_{LV}/dT$ (ergs/cm <sup>2</sup> /°C)
Al	866	- 0.50
Cu	1300	- 0.45
Au	1140	- 0.52
Fe	1880	- 0.43
Ni	1780	- 1.2
Si	730	- 0.10
Ag	895	- 0.30
Ta	2150	- 0.25
Ti	1650	- 0.26
Au <sub>0.6</sub> Ge <sub>0.4</sub> [2]	750	- 0.20

## REFERENCE

- [1] L.E. Murr, *Interfacial Phenomena in Metals and Alloys* (Addison-Wesley, Reading, MA, 1975).
- [2] Yu. V. Naidich, V. M. Perevertailo, and L. P. Obushchak, *Institute of Materials Science, Academy of Sciences of the Ukrainian SSR. Translated from Poroshkovaya Metallurgiya*, No. 5 (149), pp. 73-75, May, 1975.



# CURRICULUM VITAE

December 7.2009

## PERSONAL BRIEF

**Name:** Last name: Seungjun, Family name: Oh  
**Date of Birth:** 19. Feb. 1984  
**Nationality:** Republic of Korea  
**Sex:** Male (single)  
**Address:** 101-1 Dong Eden Village, Hadan 2 Dong,  
Saha-ku, Busan, 604-022, Korea  
**Affiliation:** Major of Semiconductor physics, Korea  
Maritime University  
**Position:** Master's course student, Department of Semiconductor  
physics  
**Office Address:** Dongsam-dong 1, Youngdo-ku, Busan, 606-791, Korea  
Tel: +82-51-410-4833, Fax: +82-51-410-4833  
**E-mail:** seung-junoh@hhu.ac.kr



## EDUCATION

**1999. 3 ~ 2002.2** Kyungnam High school, Busan, Korea  
**2002. 3 ~ 2008.2** B.S. in Semiconductor Physics, Korea Maritime University,  
Korea,  
Thesis: 'Synthesis of GaZnO nanostructures'  
**2008. 3 ~ Now** Master's course student, Department of Semiconductor  
physics, Graduate school, Korea Maritime University, Korea

## MILITARY SERVICE

**2004.3 ~ 2006.3** Republic of Korea Army (sergeant discharge)



## ACADEMIC ACTIVITIES

### (1) CAREER

**2007.6.19 ~ 2007.6.22** Completion of a course of 1<sup>st</sup> R&D Business Strategy from Ministry of Science and Technology

**2008.4** Awarded an excellent paper prize by the research institute of industrial Technology in Korea

**2008.10 ~ 2009.4** A special research student by Japan Student Services Organization in Kagawa University, Kagawa, Japan  
Academic adviser: Prof. Kensho Okamoto  
Research topic: Study on reciprocal optical transmitter using LED

### (2) PUBLICATION

- ① Microstructure evolution of highly Ga-doped ZnO nanocrystals, S. J. Oh, M. N. Jung, S. Y. Ha, S. G. Choi, J. J. Kim, K. Kobayashi, S. T. Lee, H. C. Lee, Y. R. Cho, T. Yao, J. H. Chang, **Physica E** **41** (2008) 31
- ② Investigations of the Growth Conditions and the Structural Evolution of Ga-doped ZnO Nanocrystals, S. J. Oh, M. N. Jung, S. Y. Ha, S. G. Choi, J. J. Kim, K. Kobayashi, S. T. Lee, H. C. Lee, Y. R. Cho, T. Yao, **Sae Mulli** **56** (2008) 303
- ③ Microstructure Evolution of Highly Ga-doped ZnO nanocrystals, S. J. Oh, M. N. Jung, S. Y. Ha, S. G. Choi, J. H. Chang, S. T. Lee, H. C. Lee, Y. R. Cho, **Journal of the Research Institute of Industrial Technology** **25** (2008) 15
- ④ Localization of the excitonic luminescence of ZnO nano-tetrapods, M. N. Jung, S. H. Park, S. Y. Ha, S. J. Oh, Y. R. Cho, J. S. Park, I. H. Im, B. H. Koo, T. Yao and J. H. Chang, **Physica E** **40** (2008) 2761
- ⑤ Influence of growth mode on the structural, optical, and electrical properties of In-doped ZnO nanorods, M. N. Jung, J. E. Koo, S.J. Oh, B. W. Lee, W. J. Lee, S. H. Ha, Y. R. Cho, and J. H. Chang, **Applied Physics Letter** **94** (2009) 041906
- ⑥ One-step formation of ZnO nanorod bridge structure using geminated Si substrates by vapor phase transportation, M. N. Jung, S. J. Oh, J. E. Koo, S. N. Yi, B. W. Lee, W. J. Lee, D. C. Oh, T. Yao, J. H. Chang, **Current Applied**

**Physics 9** (2009) e161

- ⑦ Investigation on the electronic state of In-doped ZnO nanocrystals by hard X-ray photoemission spectroscopy, M. N. Jung, S. Y. Ha, S. J. Oh, J. E. Koo, J. J. Kim, K. Kobayashi, Y. Murakami, T. I. Jeon, T. Yao, J. H. Chang, **Current Applied Physics 9** (2009) e165
- ⑧ Field emission properties of indium-doped ZnO tetrapods, M. N. Jung, S. H. Ha, S. J. Oh, J. E. Koo, Y. R. Cho, H. C. Lee, S. T. Lee, T. I. Jeon, H. Makino, J. H. Chang, **Current Applied Physics 9** (2009) e169
- ⑨ Structural, Optical, and Electrical properties of ZnO:Al Nanorods grown by Using a AuGe Catalyst, S. N. Kim, M. N. Jung, S. J. Oh, J. E. Koo, I. H. Heo, H. S. Ahn, S. N. Yi, J. H. Chang, H. J. Jung, B. W. Lee, H. H. Hwang, W. J. Lee, **Sae Mulli 57** (2008) 238
- ⑩ Growth Mechanism of ZnO:In Nanorods and Application as Field Emission Device, J. E. Koo, M. N. Jung, S. J. Oh, S. N. Kim, S. N. Yi, J. H. Chang, S. H. Ha, Y. R. Cho, W. J. Lee, **Sae Mulli 57** (2008) 231

### **(3) PRESENTATIONS IN CONFERENCES**

- ① Growth of  $Zn_xGa_{1-x}O$  ( $0 < x < 1$ ) Nano-Crystals; Composition Control and Field Emitter Applications, S. J. Oh, M. N. Jung, S. Y. Ha, S. G. Choi, S. H. Ha, T. Yao and J. H. Chang, (The 13th International Conference on  $\Pi$ -VI Compounds, 2007. 09, Jeju-island in Korea)
- ② Kinetic model for the growth of ZnO nanorods on various substrates, S. J. Oh, S. G. Choi, M. N. Jung, and J. H. Chang, (Nano Korea 2008 Symposium, 2008. 04, Kintex in Korea)
- ③ Growth of Well-Aligned ZnO Nanorods on ITO glass, S. J. Oh, S. G. Choi, M. N. Jung, H. H. Hwang, W. J. Lee, H. J. Jung, B. W. Lee, S. Y. Yi, and J. H. Chang, (2008 the Korea Physical Society, 2008. 04, Daejeon in Korea)
- ④ Investigation on morphological and structural evolution of Ga-doped ZnO Nanocrystals, S. J. Oh, M. N. Jung, S. Y. Ha, J. J. Kim, K. Kobayashi, S. G. Choi, H. C. Lee, S. T. Lee, Y. R. Cho, T. Yao, and J. H. Chang, (2007 Material Research Society of Korea, 2007. 11, Suwon in Korea)
- ⑤ The simplest signal transmitter using only LED, S. J. Oh, J. H. Chang, and K. Okamoto, (2009 the Korea Physical Society, 2009. 04, Daejeon in Korea)
- ⑥ Optical and Electrical Properties of InZnO Nano-Crystals, M. N. Jung, S. Y. Ha,

- S. G. Choi, S. H. Ha, S. J. Oh, T. I. Jeon, J. J. Kim, Y. Murakami, T. Yao and J. H. Chang, (The 13th International Conference on  $\text{II-VI}$  Compounds, 2007. 09, Jeju-island in Korea)
- ⑦ Evaluation of the Feasibility of Various ZnO Based Nano-Crystal for the Application to FED, S. H. Ha, M. N. Jung, S. Y. Ha, S. G. Choi, S. J. Oh, W. Lee, H. C. Lee, Y. R. Cho, Y. J. An, T. Yao and J. H. Chang, (The 13th International Conference on  $\text{II-VI}$  Compounds, 2007. 09, Jeju-island in Korea)
- ⑧ Hard X-ray Photoemission spectroscopy of  $\text{MZnO}$  ( $M=\text{In, Ga}$ ) nano-crystals, S. Y. Ha, M. N. Jung, S. J. Oh, J. J. Kim, K. Yang, E. Ikenaga, K. Kobayashi, S. Ueda, H. Yoshikawa, D. Nomoto and J. H. Chang, (The 13th International Conference on  $\text{II-VI}$  Compounds, 2007. 09, Jeju-island in Korea)
- ⑨ Realization of Field Emitter by using In-doped ZnO Nano-crystals, M. N. Jung, S. H. Ha, S. J. Oh, Y. R. Cho, G. S. Kil, T. I. Jeon and J. H. Chang, (2007 Material Research Society of Korea, 2007. 11, Suwon in Korea)
- ⑩ Feasibility of ZnO:In Nanocrystals as a Cathode Material for Field Emitting Device, J. H. Chang, M. N. Hung, S. J. Oh, Y. R. Cho, T. I. Jeon, H. Makino, Y. Murakami and T. Yao, (2008 the Korea Physical Society, 2008. 04, Daejeon in Korea)

#### **(4) PATENT**

- ① A vehicle collision avoidance system using light emitting diode, J. H. Chang, K. Okamoto, S. J. Oh, S. Y. Kim, M. N. Jung, (Patent pending, Korea)

### **LANGUAGE**

- ① Test of English for International Communication (TOEIC): 700 (Valid until 2010/03/22)
- ② TOEIC Speaking: Level 6 (Valid until 2011/08/23)
- ③ Japanese-Language Proficiency of Test (JLPT): Level 1

## 감사의 글

벌써 연구실 생활을 시작한지도 3년 반이라는 시간이 지났습니다. 그 동안 저의 인생에서 귀중한 것들을 배울 수 있었습니다. 그 중심에는 저를 지도해주신 장지호 교수님이 계십니다. 때로는 엄하게 학문적 깊이를 보여주시며, 때로는 자상하게 보듬어주신 장지호 교수님께 감사의 말씀을 올립니다. 학문적인 지식뿐만 아니라, 사람이 살아가는데 있어 중요한 것들을 많이 배웠습니다. 비록 모자라지만 부끄럽지 않은 제자가 되도록 노력하겠습니다. 또한, 많은 관심과 격려, 그리고 학문적 지도를 주신 이삼녕 교수님, 양민 교수님, 안형수 교수님, 김홍승 교수님께 감사의 말씀을 올립니다. 또한, 일본 생활을 무사히 잘 해낼 수 있도록 도와주시고 많은 재미난 연구를 가르쳐 주신 Okamoto 교수님께 감사의 말씀을 올립니다. 연구뿐만 아니라 유학생생활을 아주 보람차게 보낼 수 있도록 많은 도움을 주셔서 감사합니다. 그리고 석사생활에 어려움이 없도록 많은 도움을 주신 이봉춘 조교님과 유학생생활을 무사히 마칠 수 있도록 도움을 주신 Nishioka 님께 감사드립니다. 그리고 함께 연구하고 고생하며 서로 격려해주는 우리 나노소재 연구실의 미나 선배와 웅 선배, 선여, 그리고 성국 선배께 그리고 시영이, 진엽이, 지은이와 영지에게 감사의 마음을 전합니다.

마지막으로 그 무엇보다 지금까지 저를 키워주시고 사랑해주신 자상하고 현명하신 어머니와 온화하고 헌신을 아끼지 않는 세상 누구 보다 강한 아버지께 감사의 말씀을 올립니다.